Anurans from the Early Cretaceous Lagerstätte of Las Hoyas, Spain: New evidence on the Mesozoic diversification of crown-clade Anura

Ana María Báez

CONICET, Department of Geology, Facultad de Ciencias Exactas y Naturales, Universidad de Buenos Aires, Pabellón 2, Ciudad Universitaria, 1428 Buenos Aires, Argentina

ARTICLE INFO

ABSTRACT

The late Barremian laminated limestones of Las Hoyas in eastern Spain are famous for the large number, diversity, and quality of the fossils that they have yielded. Herein, anuran remains from these beds representing two new taxa are thoroughly described. *Iberobatrachus angelae* gen. et sp. nov. is characterized by a skull nearly as long as it is wide, a narrow neurocranium, frontoparietals fused at least along the posterior half of the orbital length, a distinct palatine process on maxilla, and moderately expanded sacral diapophyses. In turn, *Gracilibatrachus avallei* gen. et sp. nov. is characterized by a combination of characters that includes an azygous frontoparietal, eight presacral vertebrae, a monovertebral sacrum bearing narrow diapophyses, a bicondylar sacro-urostylar articulation, highly elongate metacarpals, and long distal manual phalanges. The anatomical evidence retrieved in this study is used to explore the taxonomic positions of the new taxa through a maximum parsimony analysis. This analysis supports the placement of *I. angelae* within Costata close to the extant genus *Discoglossus*, whereas *G. avallei* is nested within Xenoanura, as a basal pipimorph. These records corroborate that diversification of costatan and xenoanuran "archaeobatrachian" lineages were already well underway by the Early Cretaceous.

© 2012 Elsevier Ltd. All rights reserved.

1. Introduction

Anurans constitute a speciose and broadly distributed clade of terrestrial vertebrates today, which comprises nearly 6000 species. However, anuran remains are scarce throughout the geological record and this paucity, in combination with the fragmentary condition of most finds, diminishes the potential input of the fossil record to unravel the history of frogs. Even so, available paleontological evidence documents the appearance of major anuran lineages in the Jurassic or Cretaceous (Evans and Milner, 1993; Henrici, 1998; Gao and Wang, 2001; Báez et al., 2009). Although the divergence of these lineages must have actually preceded the earliest known records, there is no consensus on the timing of the initial splitting within the crown-group estimated by calibrated molecular clock analyses. Some of these studies propose an early divergence of the main anuran lineages in the late Permian and Triassic (San Mauro et al., 2005) or within the Triassic (Roelants et al., 2007), whereas others suggest that most of these events occurred in the Jurassic (San Mauro, 2010).

Herein several anuran specimens discovered in the Early Cretaceous Las Hoyas fossiliferous deposits of east-central Spain are thoroughly described. These deposits are famous for the large number, diversity, and exceptional quality of the remains that they have produced and, thus, they have been considered one of the most important Mesozoic Konservat Lagersttäten in the world (Sanz et al., 1988). Remains of plants, invertebrates, and vertebrates have been recovered from the rhythmically laminated limestones of the Barremian La Huérguina Formation (Fig. 1), which are part of a sequence that represents a regional scale, complex wetland ecosystem (Gómez Fernández and Meléndez, 1991; Buatois et al., 2000; Buscalioni and Fregenal-Martínez, 2010). Despite the abundance of lacustrine strata, however, anuran remains are comparatively rare.

This paper focuses on the description of several specimens mentioned previously as "Las Hoyas 1" and "Las Hoyas 2" by Báez (in press). They represent two new taxa which are formally recognized herein. The anatomical evidence retrieved in this study is used to explore their taxonomic position through a maximum parsimony analysis. Preliminary considerations of the relationships and significance of this material are also presented.

2. Materials and methods

This study is based on the examination of 9 specimens of particular anatomical and taxonomic interest, some of which are preserved as part and counterpart on two slabs. Additional specimens from the same locality still under study might represent other taxa. The
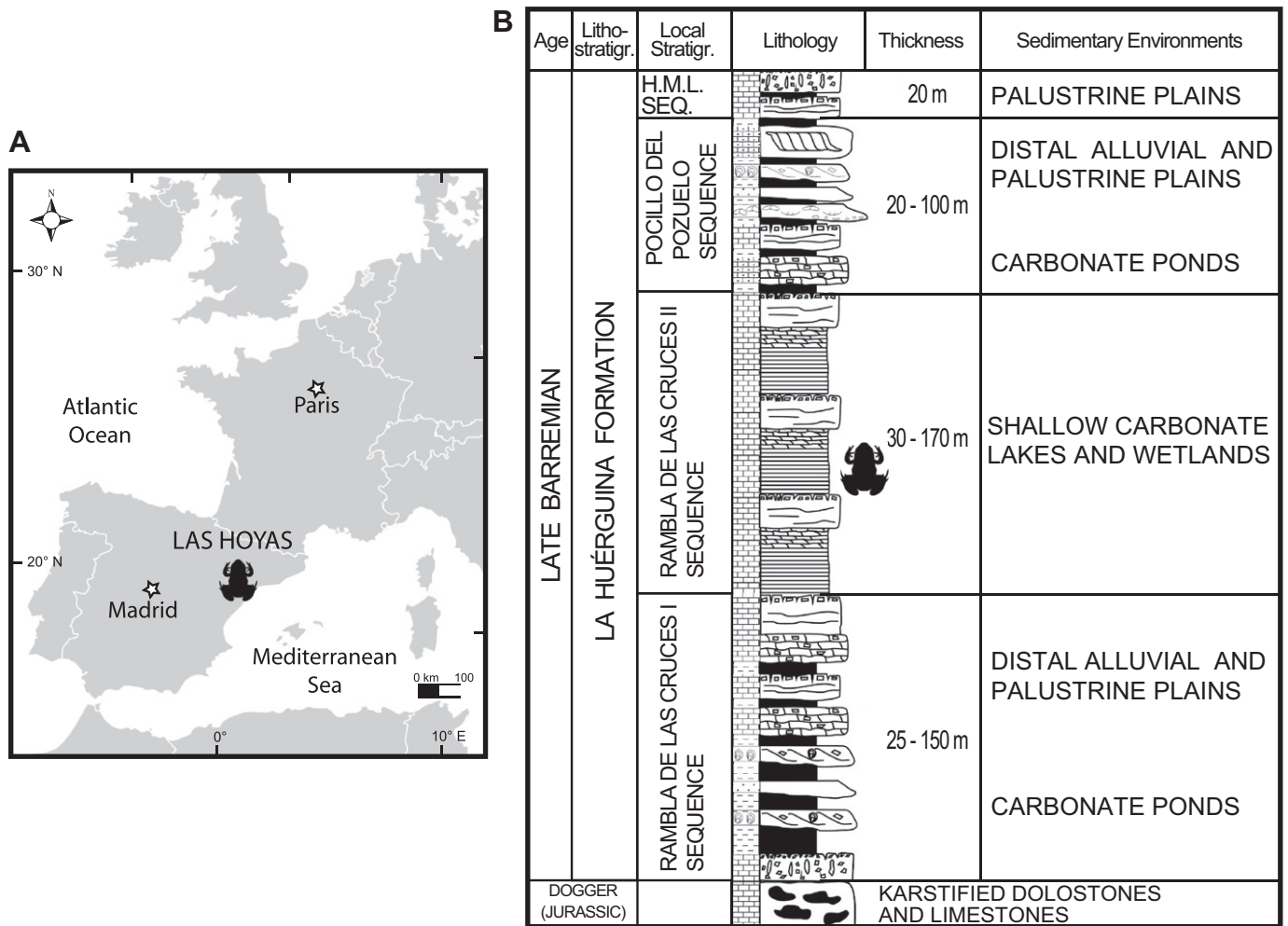
Fig. 1. A, location of the Las Hoyas fossil site in the Iberian Peninsula. B, stratigraphy of the deposits of the La Huérguina Formation indicating the frog-bearing levels. (Modified from Fregenal-Martínez and Buscalioni, 2009). Abbreviations: H.M.L. SEQ: Hoya de la Madre de las Latas Sequence.

material described herein was collected in several fieldtrips and is stored at the Museo de Ciencias de Castilla-La Mancha, Cuenca, Spain (MCCM). Most of these specimens are two-dimensionally preserved; bones are usually incomplete and split in different planes, whereas they may be also preserved as impressions, as detailed below. The osteological nomenclature follows that of Trueb (1973, 1993), Roček (1980, 2003a), and Fabrezi and Alberch (1996). The taxonomy follows the proposal of Frost (2011), which is generally consistent with the result of a broad-scale phylogenetic analysis of extant amphibian species performed by Frost et al. (2006). This comprehensive analysis was based on DNA sequence data from mitochondrial and nuclear genes combined with anatomical evidence mainly from larval structures provided by the work of Haas (2003). With regard to the higher level taxonomy, it is noteworthy that the position of the Costata as sister group of acosmanurans (Anomocoela + Neobatrachia) proposed by Frost et al. (2006) differs from that retrieved in other molecular studies (e.g., San Mauro et al., 2005; Roelants et al., 2007; Pyron and Wiens, 2011), in which Costata is the sister group of all other anurans to the exclusion of leiopelmatids. Also, it should be noted that the names proposed by Frost et al. (2006) for clades within Anura are used as stem-based names herein, except in the case of the xenoanuran lineage that includes taxa more closely related to Pipidae than to Rhinophrynidae, for which the name Pipimorpha proposed by Ford and Cannatella (1993) is accepted. Pipidae, in turn, is used for the common ancestor of living pipids and all of its descendants.

Relationships of the taxa represented by the specimens studied herein are considered in the context of the taxonomic hypothesis that results from a maximum parsimony analysis conducted using T.N.T version 1.1, as discussed below.

3. Systematic paleontology

ANURA Fischer von Waldheim, 1813
COSTATA Lataste, 1879

Iberobatrachus gen. nov.

Derivation of name. From Iberia, the ancient name of the peninsula now comprising Spain and Portugal where the type locality is located, and batrachos, meaning frog in Greek.

Type species. Iberobatrachus angelae gen. et sp. nov.

Diagnosis. As for the only known species.

Iberobatrachus angelae sp. nov.

Derivation of name. The specific epithet is dedicated to Angela Delgado Buscalioni, paleontologist and professor at the Universidad Autónoma de Madrid, Spain, for her contribution to the knowledge of the Las Hoyas fossil site.

Holotype. MCCM-LH 11393a–b; articulated specimen lacking the hindlimbs and left forelimb, two-dimensionally preserved as part and counterpart on two slabs (Fig. 2A and B).

Type locality. Las Hoyas fossil site, approximately 30 km east of Cuenca, La Cierva Township. Cuenca Province, Spain.

Stratigraphic horizon. La Huérguina Formation, upper Barremian.

Referred specimens. MCCM-LH 15999a–b; incomplete, articulated specimen preserved as part and counterpart on two slabs.

Diagnosis. Costatan frog that differs from other costatan taxa in having a narrow neurocranium, the width of which at the level of the midorbital length represents 15% of the maximum width skull and frontoparietals fused at least along the posterior half of the orbital length and forming a flat dorsal table, and also from *Alytes* and bombinatorids in the maxilla bearing a palatine process. It further differs from *Eodiscoglossus santonjae* and *Wealdenbatrachus jucarensis* in the proportions of the skull, which is as long as wide, and the more distally expanded sacral diapophyses, and from the latter also in the absence of the high dorsal crest on urostyle.

Description

This taxon is represented by two partially articulated specimens (MCCM-LH 15999a, b; 11393a, b). These specimens belong to adult individuals based on the high degree of ossification of all parts of the skeleton; they are estimated to be about 40 mm in snout-vent length. Cranial and part of the postcranial skeletons are preserved. The following description is composite and based on these two specimens, as specified below.

Cranial skeleton. One of the most characteristic features of this taxon is the distinctive triangular outline of the skull in dorsal view. The head is nearly as long as wide, with the maximum width of the skull across the otic capsules slightly shorter than the maximum median length, measured from tip of snout to occipital condyles. In addition, the braincase, measured at the level of the midlength of the orbital region, is narrow, being about 15% the maximum width of the skull. The length of the preorbital region represents 33% of the median length of the skull.

The left premaxilla is preserved in MCCM-LH 15999b, whereas this bone is not discernible in the holotype. It bears 7–8 tooth pedicels and a relatively long alary process directed dorsolaterally. The maxillae are long and well ossified; each bone extends from its articulation with the premaxilla, anteriorly, to near the level of the posterior margin of the orbit, posteriorly. Its posterior portion overlaps the quadratojugal laterally, as shown in MCCM-LH 15999a. The maxilla bears a well-developed pars facialis that is deep anterior to the orbit, moderately developed along the anterior half of the orbit, and reduced in height posterior to the articulation with the anterior ramus of the pterygoid. At the level of the anterior
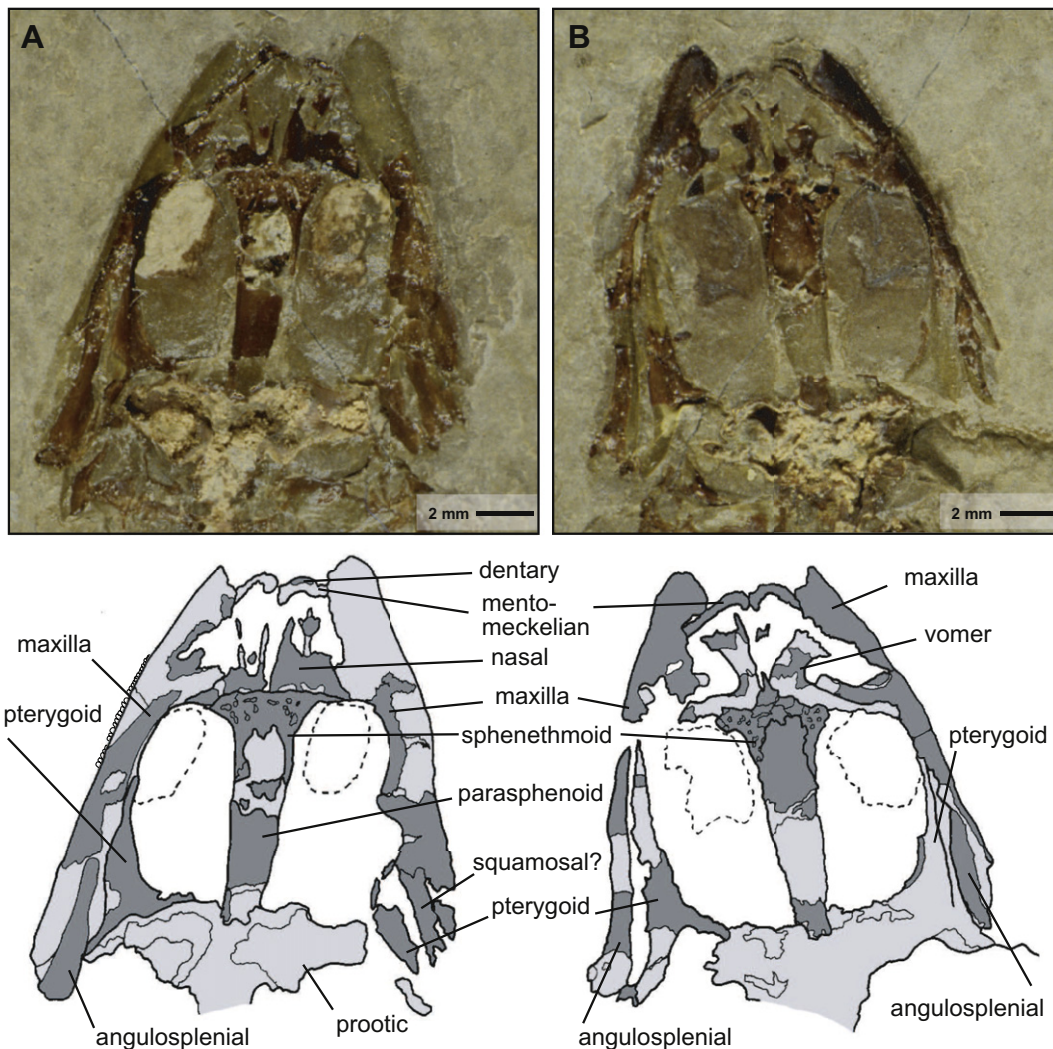
Fig. 2. *Iberobatrachus angelae*, gen. et sp. nov., holotype. A, close-up of skull (MCCM-LH 11393a); below, interpretive drawing. B, counterpart (MCCM-LH 11393b); below, interpretive drawing.

margin of the orbit, the pars facialis of the maxilla forms a distinct preorbital process discernible in both MCCM-LH 15999 and 11393 (Fig. 2A). At this level, pieces of maxilla ventral to the nasal and in contact with the vomer in the holotype indicate the presence of a maxillary palatine process. This process lies adjacent to the postchoanal process of the vomer. The disarticulated left maxilla is discernible in MCCM-LH 11393a showing the slightly concave dorsal margin of the pars facialis beneath the orbit, a shallow expansion at the point where the pterygoid contacts the maxilla, and a narrow postorbital process that suggests the maxilla was in contact with the zygomatic process of the squamosal There is no sculpturing on the dorsal surface of the maxilla. Impressions of pedicellate teeth are visible in this specimen along the maxilla up to the level of the posterior third of the orbit. A count of 36 tooth pedicels along the margin of the anterior portion of the left maxilla up to midorbit length is possible.

The well-developed quadratojugal is preserved in MCCM-LH 15999a; it articulates with the quadrate and ventral ramus of the squamosal, medially, and with the posterior process of the maxilla, laterally and anteriorly. The long pars jugalis (sensu Bolkay, 1919) of the quadratojugal extends along the posterior 55% of the pterygoid fossa.

The nasals are incompletely preserved in both specimens but the remnants of these bones indicate that they were relatively extensive, roofing most of the posterior one-half of the nasal capsules. Their straight medial margins suggest that they were very narrowly separated or in contact with each other along the midline (Figs. 2A and 3). Anteriorly, each nasal forms a short rostral process, whereas posterolaterally it extends toward the maxilla. Posteriorly, the nasals slightly overlap the ossified sphenethmoid.

The frontoparietals are incompletely and poorly preserved in the two specimens; this prevents a detailed description of the most anterior and posterior portions of these bones. In MCCM-LH 15999b, a portion of the skull roof in ventral aspect is visible in the posterior orbital region. A medial suture between left and right frontoparietals is not discernible, indicating that the parietal portions of these bones might have been fused to one another. In addition, it is clear that the frontoparietal formed the flat, parallel-sided roof of the braincase in this region, bearing a well-developed lamina perpendicularis on each side and lacking supraorbital shelves. Fragments of the frontoparietal indicate that its width increased at the level of the anterior margin of the otic capsules, where this bone invested the medial portion of these structures; however, the shape of the posterior margin is unknown.

A fragment of the cultriform process of the parasphenoid in the posterior orbital region is preserved in situ in the holotype. This fragment is relatively wide and has parallel lateral margins and a slightly convex ventral surface that would have floored the cartilaginous braincase between the bony sphenethmoid and the prootics in the living animal.

The vomers are preserved only in the holotype; these bones are exposed in dorsal view in MCCM-LH 11393b, whereas fragments and impressions are visible on the counterpart (Fig. 2B). They are extensive bones underlying the nasal capsules. The anterior terminus of each vomer lies near the palatal shelf of the maxilla, without reaching the maxillary arch, whereas its posterior terminus lies at the level of the postnasal wall. The medial margin of the plate-like portion of the vomer diverges anteriorly and laterally from the midline. Laterally, this portion surrounds the endochoanal fenestra anteriorly, medially, and posteriorly, although a circumchoanal process distinct from the plate-like portion is not evident. Owing to the dorsal exposure of the vomers, it was not possible to determine the presence of a dentigerous process.
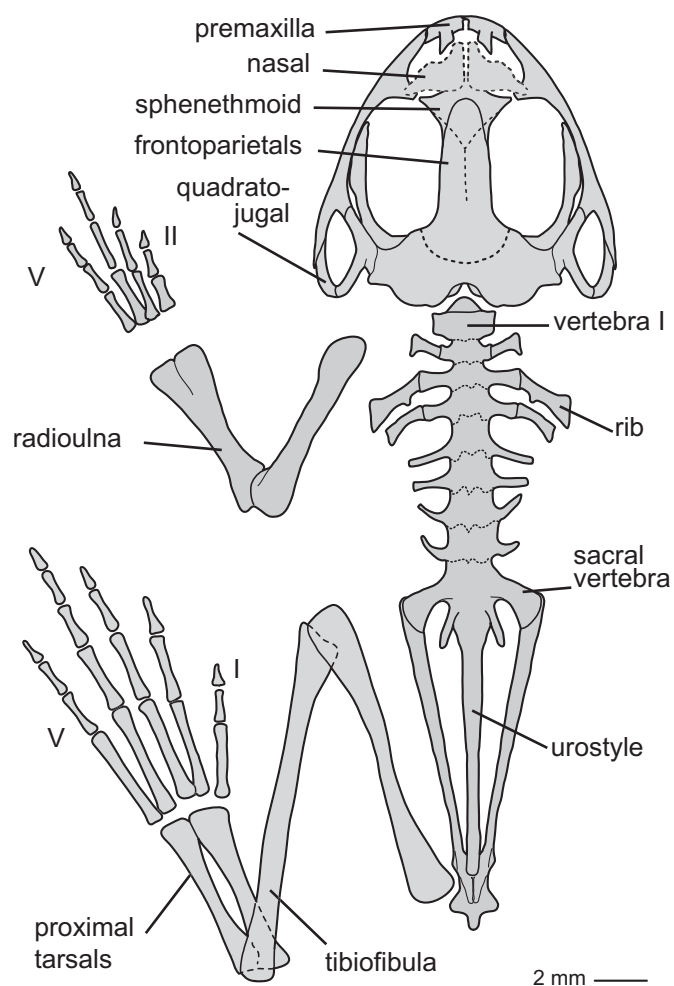
Fig.3. *Iberobatrachus angelae*, gen. et sp. nov. Partial restoration of the skeleton in dorsal aspect. Modified from Báez (in press).

Impressions and remnants of the triradiate pterygoids are preserved in the holotype and MCCM-LH 15999. The anterior ramus is long; the anterior end nearly reaches the anterior margin of the orbit. A moderately developed ventral flange on the posterolateral margin of this ramus is discernible in the holotype (Fig. 2B). The medial ramus is the shortest of the three rami of the bone; it articulates with the anterior wall of the otic capsule, but its relationship with the parasphenoid can not be assessed with the available information. The posterior ramus is directed posterolaterally and invested the medial surface of the quadrate cartilage.

The squamosals are poorly preserved and difficult to identify in the two specimens; fragments of bone that might belong to the ventral ramus of this element are visible in MCCM-LH 15999b.

The sphenethmoid is preserved in the holotype and in MCCM-LH 15999. The longitudinal section of this bone shows its cancellous texture characteristic of endochondral bone (Fig. 2A). Anteriorly, the sphenethmoidal ossification might have extended into the posterior part of the relatively narrow septum nasi, which separates the nasal capsules and terminates near the maxillary arch. Anterolaterally, the sphenethmoidal ossification invades the proximal thirds of the postnasal walls to form short anterolateral wings, indicating that the orbitonasal foramina were enclosed in bone. Dorsally, the sphenethmoid circumscribes the anterior and lateral margins of the frontoparietal fenestra. Anterodorsally, the sphenethmoid was invested by the most posterior portion of the nasals, whereas the anterior-most remains that can be attributed to the

frontoparietals lie posterior to the level of the anterior margin of the frontoparietal fenestra. This evidence suggests that there was no contact between the nasals and frontoparietals and that the sphenethmoid was probably exposed dorsally between these dermal bones. Posteriorly, the sphenethmoid reaches the level of the mid-length of the orbit (Fig. 2A and B).

Each otic capsule is formed by the synostotically fused prootic and exoccipital. The otic capsules have a rounded outline, extending laterally into a distally truncate, ossified crista parotica, the distal margin of which reaches slightly beyond the lateral margin of the orbit.

The mandible is composed of angulosplenials, dentaries and mentomeckelians. A low coronoid process is visible on the posteromedial region of the angulosplenial, whereas the expanded anterior end of the dentary in the holotype suggests the presence of a fused mentomeckelian bone. The articulation of the mandible with the skull is situated at the level of the occiput.

Postcranial skeleton. The presacral region of the axial skeleton consists of eight vertebrae that show no fusions to one another (Fig. 3). The vertebral centra are poorly preserved in the two specimens pertaining to this taxon; they are usually sectioned or missing, making it difficult to determine the configuration of the articular facets or their morphology in detail. However, the sectioned centra of presacral vertebrae II and III in MCCM-LH 15999b are anteriorly convex and posteriorly concave, indicating an opisthocoelous condition. The atlas is distinctly larger than the other presacrals in ventral view; its ventral outline suggests that the occipital cotyles were narrowly separated (type II of Lynch, 1971), although a medial notch separating the cotyles is absent. Transverse processes are not present on the atlas. The succeeding three presacrals bear transverse processes that are slightly expanded distally, particularly those on Vertebra III and IV. These transverse processes articulate with ribs that are slightly expanded proximally and distally, and slightly longer than the transverse processes with which they articulate. The

ribs on Vertebra III are longer than those on vertebrae II and IV, and bear posteriorly directed uncinate processes. The succeeding two presacrals (V and VI) have long and blunt transverse processes; those on Vertebra V may be slightly posteriorly directed, whereas those on the following vertebra (VI) are perpendicular to the longitudinal axis of the vertebral column. The transverse processes of last two presacrals (VII and VIII) are sharply pointed distally and anteriorly directed with an angle of about 70° with respect to the longitudinal axis of the column. The distances between the lateral margins of the last two presacral vertebrae are shorter than that between the lateral margins of the sacral diapophyses. The sacrum is formed by a single vertebra (Vertebra IX), which bears moderately expanded diapophyses (Fig. 4B and C). The anterior margins of the sacral diapophyses are slightly posteriorly directed, whereas the posterior margins are more markedly so; the lateral margins are convex. In the holotype the sacral vertebra articulates with the urostyle, which has a broad anterior end and bears a pair of posteriorly directed transverse processes. In MCCM-LH 15999, posterior to the sacral vertebra there is a post sacral neural arch bearing posteriorly directed, blunt transverse processes, which is followed by the broad anterior end of the urostyle (Fig. 4C). The type of articulation between the sacrum and urostyle is not clear owing to the poor preservation of this region in the specimens examined.

Disarticulated elements of the pectoral girdle are present, but poorly preserved, in the holotype and MCCM-LH 15999, both in parts and counterparts. The scapula is relatively short and in MCCM-LH 11393a a shallow notch separating the pars acromialis from the pars glenoidalis is discernible. The clavicle is incompletely preserved but it is clear that it was anteriorly bowed. The coracoid has a straight long axis; its flattened sternal end was not greatly expanded. The cleithrum is relatively large; it invested a large portion of the dorsal surface of the suprascapular cartilage in life. The dorsal margin of the cleithrum has a shallow concavity that defines a weakly bifurcate margin.
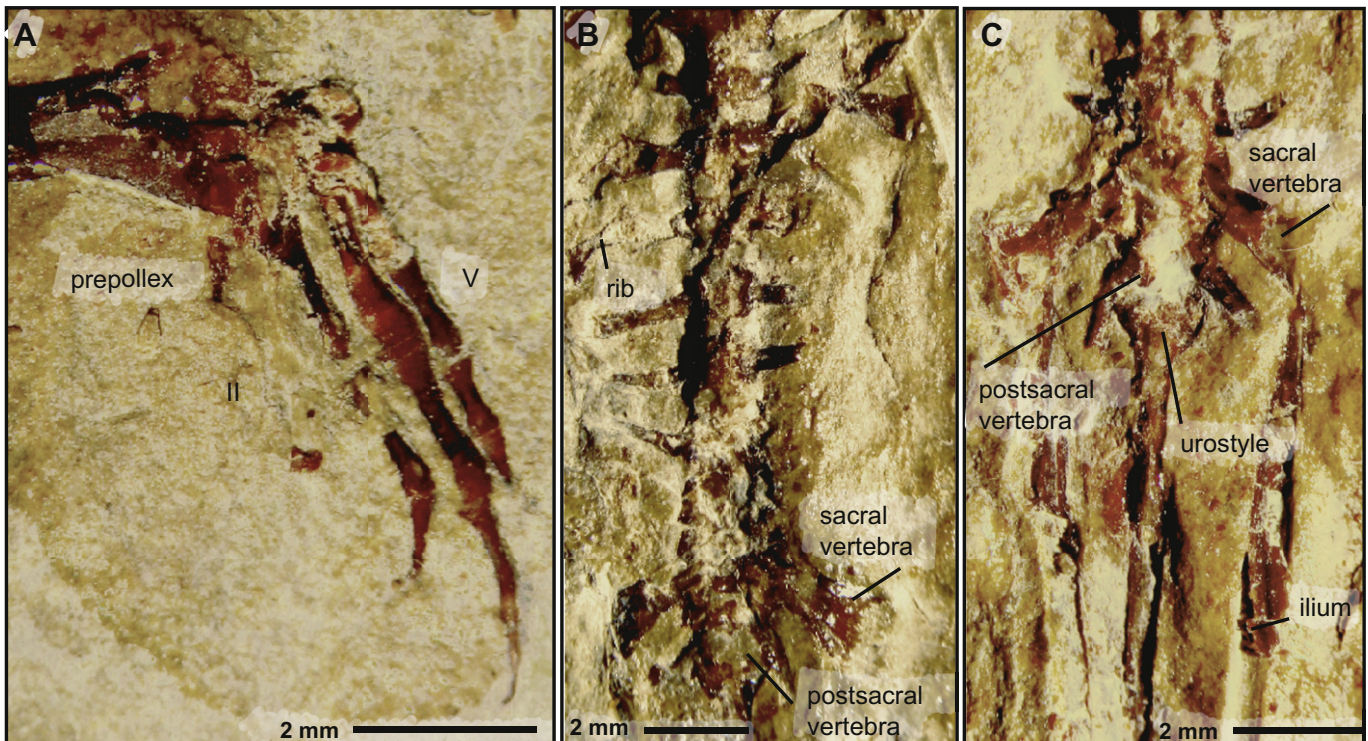
Fig. 4. *Iberobatrachus angelae*, gen. et sp. nov. A, distal portion of left forelimb (MCCM-LH 15999b). B, axial skeleton (MCCM-LH 15999a). C, sacro-urostylar region in dorsal aspect (MCCM-LH 15999b)

The left forelimb is discernible in the two specimens examined; however, the proximal portion of the humerus is obscured by elements of the pectoral girdle. Despite the poor preservation it is evident that the humeral diaphysis is not strongly recurved and that the ventral ball is well ossified. The radioulna has a well-developed olecranon process and an expanded distal end; a sulcus intermedius is discernible along the distal one-third of its length. Only a few carpal elements are preserved in situ; two large elements are present in the proximal row next to the distal end of the radioulna, probably representing the radiale and ulnare. The metacarpals are not elongated; Metacarpal II is distinctly more robust than the others. The phalangeal formula is 2233. The terminal phalanges are pointed.

The pelvic girdle and hind limb are preserved in MCCM-LH 15999. The ilia have long, straight shafts that show no evidence of the presence of dorsal crests. The femur is incompletely preserved but it is clear that it was a sigmoid bone shorter than the tibiofibula. The expanded proximal and distal ends of the tibiale and fibulare are in contact but not fused to one another. Their total length represents 48% of the length of the tibiofibula. The longest metatarsal is MIV, which is 60% of the length of the proximal tarsals. The distal tarsals are not preserved; these elements might have been cartilaginous. The terminal phalanges are distally pointed.

Remarks. The specimens described here have been briefly considered by Báez (in press) as "Las Hoyas 2". The presence, in combination, of eight discrete presacral vertebrae, free short ribs on presacrals II, III, and IV, sacrum not fused to the urostyle and transverse processes on the urostyle in adults of *Iberobatrachus angelae* is generally consistent with costatan affinities. This lineage of basal anurans is represented today by the genera *Alytes* Wagler 1829, *Barbourula* Taylor and Noble 1924, *Bombina* Oken 1816, and *Discoglossus* Otth 1837, all distributed within the Palearctic region. These taxa form a well-corroborated clade in most recent phylogenetic analyses based mainly on DNA sequence data (San Mauro et al., 2005; Frost et al., 2006; Blackburn et al., 2010; Pyron and Wiens, 2011), which also support the division of this clade into two subclades: Alytidae (including *Alytes* and *Discoglossus*) and Bombinatoridae (including *Bombina* and *Barbourula*). The lineage to which these genera belong is considered one of the earliest diverging anuran lineages, dating back at least to the Jurassic (Sanchiz, 1998). However, several of the Jurassic and Cretaceous taxa considered to be members of the costatan lineage are represented by isolated bones or poorly preserved specimens and their phylogenetic placement is still ambiguous (e.g., Evans and McGowan, 2002; Gao and Chen, 2004). Comparisons of *I. angelae* with the putative costatans *Eodiscoglossus santonjae* Vidal, 1954 and *Wealdenbatrachus jucarensis* Fey, 1988 from the Barremian of northeastern Spain appear pertinent owing to their geographic and temporal proximity, although the disparate preservation of the available specimens precludes detailed assessment of their osteological features. *Eodiscoglossus santonjae* is based on a two-dimensionally preserved, articulated specimen, (MNCN 4723) of approximately 28 mm in snout-vent length exposed mainly in dorsal view (Hecht, 1970; Estes and Reig, 1973). Other incompletely preserved materials have been referred to the same species, but my comments are based on the examination of the holotype. In turn, *W. jucarensis* is known from disarticulated, three-dimensionally preserved remains that belong to an individual of nearly 60 mm of snout-vent length, described and assigned with doubt to the Costata ("Discoglossidae" therein) by Fey (1988), but subsequently considered to represent a close relative of *Discoglossus* by Sanchiz (1998) The outline of the skull of *I. angelae* is distinctly different from those of these two Cretaceous taxa. The skull is nearly as long as wide in *I. angelae* whereas

is wider than long in both *E. santonjae* and *W. jucarensis*, which also have more broadly arched jaws. The long and straight anterior ramus and short medial ramus of the pterygoid in *I angelae* contrasts with the more laterally directed anterior ramus and long medial ramus of the pterygoid of *W. jucarensis*. The elongate frontoparietal fontanelle that reaches the level of the posterior margin of the orbit described for the latter taxon (Fey, 1988) differs from the fused frontoparietals forming a flat dorsal surface for most of the orbital region in *I. angelae*. In the latter species, the sphenethmoidal ossification extends anterolaterally and into the posterior portion of the nasal septum, this condition is unlike the short, anteriorly blunt sphenethmoid of *E. santonjae*, although this difference might be the result of ontogenetic bias. Although the articulation of the zygomatic process of the squamosal with the maxilla was figured by Roček (2000), this condition is not present in the holotype of *E. santonjae* according to my observations, whereas the presence of a zygomatic process on the maxilla in *I. angelae*, absent in *Wealdenbatrachus*, indicates that the maxilla articulated with the squamosal in *I. angelae*. The sacral diapophyses of the latter species are moderately expanded and only slightly posteriorly directed, thus differing from the narrow, posteriorly angled sacral diapophyses of *W. jucarensis* (Fey, 1988). In turn, photographs of the sacral region of the holotype of *E. santonjae* taken under polarized light and published by Hecht (1970) clearly show narrow sacral diapophyses, contra the opinion of Gao and Wang (2001) who scored the sacral diapophyses for *Eodiscoglossus* as expanded. There is no evidence of a high dorsal crest on the urostyle in *I. angelae*, whereas this feature is clearly present in *Wealdenbatrachus*. In addition, a distinct dorsal crest on the iliac shaft is lacking in *I. angelae*, unlike the condition in *Wealdenbatrachus*. The proportions of the zeugopodial and stylopodial components of the hind limb of *Iberobatrachus* resemble those *Wealdenbatrachus*, differing from those of *E. santonjae* in which the femur is nearly as long as the tibiofibula instead of being shorter than the latter bone. In *I. angelae* the proximal tarsals are not extensively fused proximally and distally to one another as in *Wealdenbatrachus* (Fey, 1988). All this morphological evidence clearly supports the conclusion that the specimens MCCM-LH 13393 and 15999 are referable to a taxon distinct from *Eodiscoglossus santonjae* and *Wealdenbatrachus jucarensis*. The new taxon, *Iberobatrachus angelae*, also differs from the Early Cretaceous *Callobatrachus sanyanensis* from northeastern China (Wang and Gao, 1999; Gao and Wang, 2001), a poorly preserved putative member of a polytomy that also includes the extant costatan genera and *Eodiscoglossus* according to the analysis by Gao and Chen (2004). *Iberobatrachus angelae* differs strikingly from *Callobatrachus* in having a skull with a more acute snout, lower number of premaxillary (and probably maxillary) teeth, an azygous skull table in the posterior orbital region formed by the fused frontoparietals instead of having paired frontoparietals, eight presacral vertebrae instead of nine, less expanded sacral diapophyses, and cleithrum with a shallow indentation on its distal margin, which is lacking in the Chinese species. The putative costatan *Bakonybatrachus fedori* from the Upper Cretaceous of Hungary, recently described by Szentesi and Venczel (2012), is known by an incomplete ilium, which bears a high dorsal crest unlike the ilium of *I. angelae*.

XENOANURA Savage, 1973
PIPIMORPHA Ford and Cannatella, 1993

Gracilibatrachus gen. nov.

Derivation of name. From the Greek gracile and batrachos, frog, in reference to the slender skeleton.

Type species. G. *avallei* gen. et sp. nov.
Distribution. Lower Cretaceous of Spain
Diagnosis. As for the only known species.

Gracilibatrachus avallei sp. nov.

Derivation of name. The specific epithet is dedicated to the Spanish herpetologist Borja Sanchiz Gil de Avalle for his important contribution to the knowledge of fossil and living anurans.
Holotype. Specimen MCCM-LH 21171a, b, Museo de Ciencias de Castilla-La Mancha; articulated skeleton of a postmetamorphic individual (Fig. 5A) preserved as part and counterpart on two slabs.
Type Locality. Las Hoyas fossil site, approximately 30 km east of Cuenca, La Cierva Township, Cuenca Province, Spain.
*Stratigraphic horizon.* La Huérguina Formation, upper Barremian.
Diagnosis. Small pipimorph xenoanuran differing from *Neusibatrachus wilferti* in the absence of quadratojugal, presence of eight presacral vertebrae, the two most posterior of which bear short, acuminate transverse processes, sternal end of coracoid moderately expanded, and femur longer than tibiofibula. It differs from all known palaeobatrachids in the absence of a synsacrum formed by

V7, V8, and V9 and presence of perichordal vertebrae, and from *Thoraciliacus*, *Cordicephalus*, and crown pipids in the presence of mentomeckelian bones, dentate vomers (except some species of *Xenopus*), and narrow sacral diapophyses, and from all crown pipids in the T-shaped squamosal and bicondylar articulation between sacrum and urostyle
Referred Specimens. MCCMLH-17422a, b, 11386, 11387, 26251, 26803a, b (in part), and, tentatively, 11394a, b.
Description of the holotype

The specimen MCCM-LH-21171 consists of the almost fully articulated skeleton of a single individual; it is two-dimensionally preserved on one slab and its counterpart. The snout-vent length is estimated to have been about 20.5 mm. The well-ossified bones of the skull and postcranial skeleton suggest that it belongs to an individual that has completed metamorphosis. However, although the ribs are fused to the corresponding transverse processes on the anterior presacral vertebrae, the swelled areas where this fusion occurred (Fig. 5C) indicate that it took place shortly before death, suggesting that the skeleton probably belongs to a juvenile. Several bones are preserved in dorsal aspect in the part (MCCM-LH 21171a), whereas other elements are exposed in ventral aspect on the
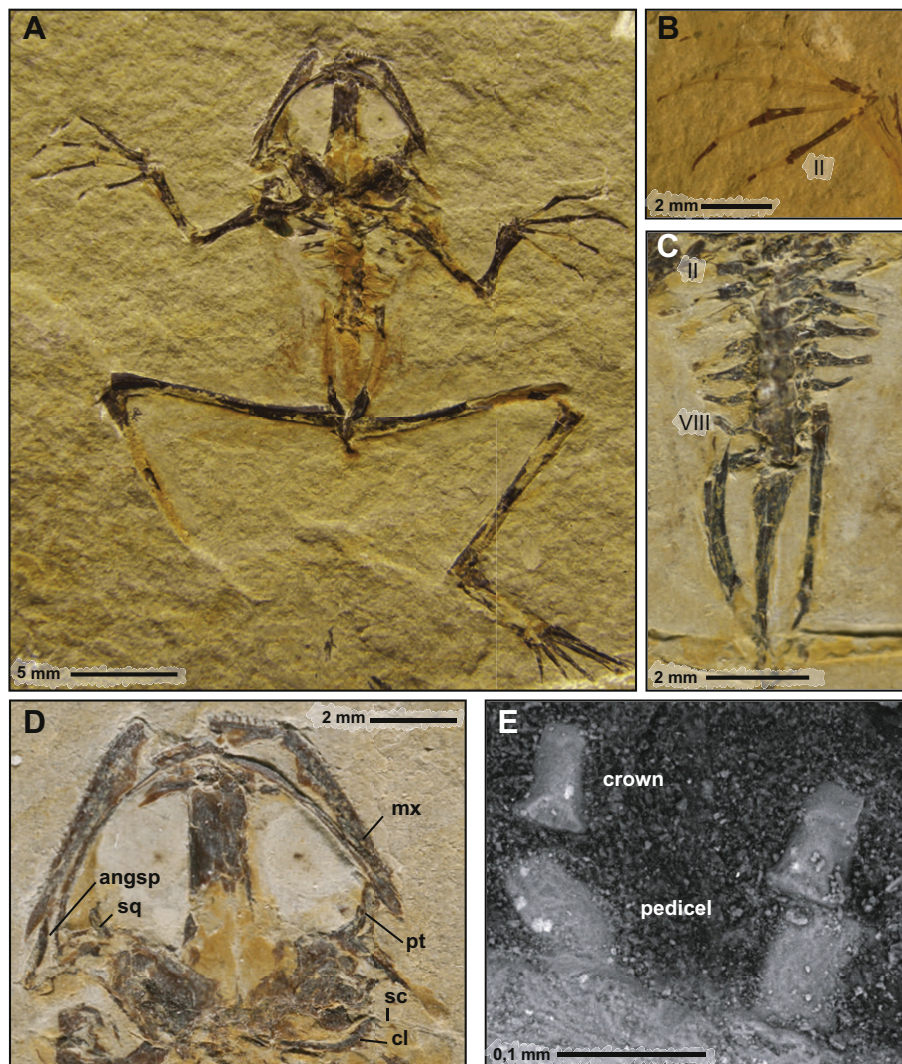
Fig. 5. *Gracilibatrachus avallei* gen. et sp. nov, holotype. A. General view of MCCM-LH 21171a. B, close-up of right hand showing the long distal phalanges (MCCM-LH 21171b). C, vertebral column and pelvis in ventral aspect (MCCM-LH 21171b). D, skull, dorsal aspect (MCCM-LH 21171a). E, close-up of pedicellate premaxillary teeth (MCCM-LH 21171a).

counterpart (MCCM-LH 21171b); dorsal and ventral impressions of other skeletal parts complete the specimen. Impressions of soft-tissue structures, such as the eyes and general body outline, are also visible (Fig. 5D).

Cranial skeleton. The skull is slightly wider than long and is widest at the level of the lower jaw articulation. The preorbital region is short (Figs. 5D and 6), its length representing 1/5 of the median length of the skull. Bones of the anterior palate, such as vomers, are fragmentarily preserved, whereas the sphenethmoid and parasphenoid are not exposed.

The paired nasals are shallow bones that probably did not roof the nasal capsules completely. The nasals are partially y preserved; this prevents detailed description of their overall shape although it is clear that they formed the greater part of the anterior margins of the orbits and may have contacted the blunt, inconspicuous pre-orbital processes of the maxillae.

The frontoparietals are fused medially along their entire length to form an azygous element. The anterior part of this element has a rounded margin and overlaps the most posterior portions of the nasals. In the orbital region, the frontoparietal overlaps the sphenethmoid, which is not exposed dorsally. The lateral margins of the frontoparietal are nearly parallel along the anterior two thirds of the orbital length and do not form supraorbital flanges. The width of the frontoparietal increases posteriorly; this expanded portion has rounded margins and invests the medial region of the otic capsules. The dorsal surface of the bone is flat.

The premaxillae are anteroposteriorly long, each bone being about 28% of the length of the maxilla; this suggests a relatively posterior position of the crista subnasalis, a block of cartilage that contributes to bracing the maxillary arch against the skull. A wide-based alary process that is located at the midlength of the bone is exposed on the right premaxilla. The pars palatina, visible on the left premaxilla, is well developed; medially it expands slightly to form a modest palatine process directed posteriorly. The pars dentalis of the right premaxilla bears about 10 teeth, whereas teeth are not preserved on the left element. The premaxillary teeth are composed of a high pedicel that protrudes from the ventral margin of the pars dentalis and a labiolingually depressed crown that bears at least one inwardly recurved cuspid. The crown is separated from the pedicel by a space that indicates that a non-mineralized zone intervened between these tooth parts (Fig. 5E).

The anterior end of the maxilla bears a short edentulous process at the level of the pars dentalis that slightly overlaps the premaxilla. The acuminate posterior end reaches close to the level of the posterior margin of the orbit and terminates freely in the absence of a quadratojugal. The maxillary pars facialis is higher at the level of the anterior margin of the orbit where it forms a rounded, relatively low antorbital process. A fine groove extends along the external surface of the pars facialis, which is otherwise flat and smooth. The maxillary arch was probably incomplete as there is no clear evidence of quadratojugal on neither side of the skull. About 19 teeth are preserved on the right maxilla and 24 on the left bone, although the total number of tooth positions is not possible to be determined because of the orientation in which the maxillae are preserved. This also prevents observation of the entire extent of the maxillary teeth, although they seem to have lower pedicels than those of the premaxillary teeth.

The squamosals are well-ossified, T-shaped bones. The free ending zygomatic ramus of each squamosal is nearly twice as long as the otic ramus. The ventral ramus, which in life invested the palatoquadrate cartilage laterally, is about three times the length of the zygomatic ramus.

The only part of the pterygoids that is clearly visible in this specimen is the anterior ramus of the left bone. This ramus is relatively long; its anterior portion gently curves medially, reaching the anterior one-third of the orbit.

The prootics form the conspicuous, rounded otic capsules, the dorsal surfaces of which are fragmented into numerous pieces of bone.

The lower jaw is composed of the angulosplenial and dentary; the presence of a mentomeckelian can not be determined with certainty. A conspicuous coronoid process is not evident. The lower jaw articulation with the skull lies at a level well anterior to the occiput.

The vomers might be represented by pieces of bone ventral to the nasals but they are too poorly preserved to be described.

The pars media plectri is the only component of the auditory apparatus for which there is some evidence. Impressions and bony remains on both sides of the skull indicate that these elements were well ossified, each consisting of a narrow stylus with an expanded proximal end.

Postcranial skeleton. Eight presacral vertebrae, the sacrum, and the urostyle comprise the vertebral column (Figs. 5C and 6). Portions of the articulated presacrals in ventral aspect are preserved in MCCM-LH 21171b, whereas the counterpart preserves this part of the skeleton mostly as impressions. The mode of articulation between successive vertebral centra is not possible to be ascertained, although the centrum of Vertebra VIII appears to bear a pair of posterior condyles, as does the centrum of the succeeding vertebra (sacral) for the articulation with the urostyle. High pedicles are discernible on both sides of each centrum along the presacral portion of the column. The atlantal centrum is shorter than the centrum of other presacrals but it does not seem to be fused to that of the succeeding vertebra; atlantal transverse processes are lacking. The transverse processes of vertebrae II and VI are laterally oriented whereas those of vertebrae III, IV and V are slightly posteriorly directed. The widths between the distal ends of contralateral processes of all these presacral vertebrae are clearly greater than that between the lateral margins of the sacral diapophyses. However, the bulky regions near the proximal ends of these processes (Fig. 5C) indicate that they have coalesced with the
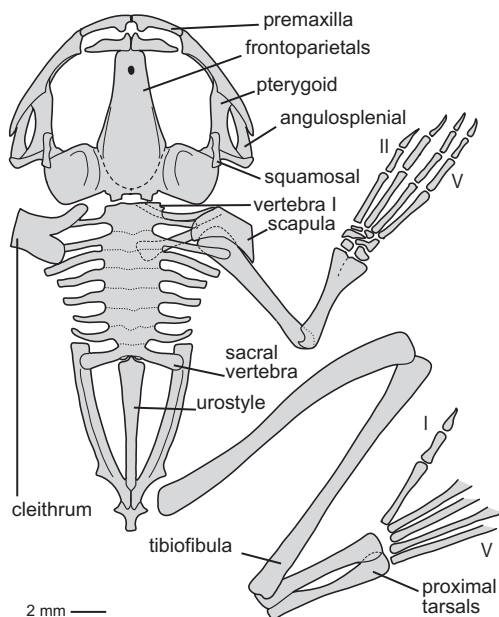
Fig. 6. *Gracilibatrachus avallei* gen. et sp. nov. Partial restoration of the skeleton in dorsal view. Modified from Báez (in press).

proximal epiphyses of the ribs according to the documented information for some living frogs (Blanco and Sanchiz, 2000). This evidence suggests the former presence of 5 pairs of ribs on vertebrae II–VI during development. In contrast, there is no evidence that ribs are attached to the transverse processes of the posterior two presacrals. Vertebra VII bears slightly anteriorly curved transverse processes that are more delicate than those on the preceding vertebrae. The right transverse process of Vertebra VIII is also anteriorly curved but that on the left side is somewhat expanded and articulates with the ilium. The relative lengths of the transverse processes in descending order are: III-IV-V-VI-II-VII-VIII, in which the numbers denote the vertebra on which they are borne. The sacral diapophyses are narrow and slightly directed posteriorly. The length of the urostyle is equivalent to that of the anterior seven presacrals. The anterior portion of the urostyle is relatively wide (Fig. 5C), but no transverse processes are discernible. There is no evidence of post sacral vertebrae.

The pectoral girdle probably was arciferal based on the morphology and disposition of preserved components The pars acromialis of each scapula articulates with the strongly curved, expanded dorsal end of the clavicle, whereas the pars glenoidalis articulates with the coracoid; the presence of a proximal notch separating these pars of the relatively short scapula could not be determined in this specimen. The anterior margin of the scapular shaft is straight owing to the presence of an anterior lamina that extends from the pars acromialis to the anterodorsal corner of the bone. The distal margin of the scapula articulated with the suprascapular cartilage, the proximal portion of which was invested dorsally by the conspicuous cleithrum (Fig. 5A). The latter bone bears a curved, anteriorly directed process that probably surrounded the anterior margin of the suprascapular cartilage, and a shorter posterior tongue-like projection. The preserved portion of the right clavicle indicates that it was an anteriorly bowed bone with a curved, pointed, distal end, but its articulation with the scapula is not clearly exposed. The glenoidal end of the coracoid is less expanded than the sternal end. The humerus is well ossified and relatively straight. The radioulna is about 71% the length of the humerus; its proximal end bears an olecranon process, whereas its distal end is expanded. Few components of the carpus are preserved. Two carpal elements are clearly visible in the right limb: a bone with a trapezoidal cross-section, which might be the ulnare, is preserved in contact with the distal end of the radioulna, and another bone articulated distally with the ulnare and in contact with the base of Metacarpal V, which might be Distal Carpal V. The metacarpals are slender bones, not widely expanded proximally or distally (Fig. 5A and B), with their lengths (in ascending order) being II < IV = V < III. The length of Metacarpal III is nearly 70% of the total length of the radioulna. The phalangeal formula is 2233; the distal phalanges are delicate and notably long, particularly those of the inner two digits (Fig. 5B).

The posterior part of the pelvic girdle is preserved in dorsal view on one of the slabs (MCCM-LH 21171a), although the broken iliac shafts are rotated along their longitudinal axes exposing their internal sides. In turn, the iliac shafts anterior to the acetabula are preserved in ventral aspect on the counterpart. The iliac shafts are as long as the presacral vertebrae plus the sacrum; when in natural position their internal margins formed a narrow angle. A low, but distinct, crest extends along the dorsal margin of the shafts; a projecting dorsal prominence is not evident. Well-developed preacetabular expansions are present, whereas the presence of an interiliac tubercle could not be ascertained. The ischia are robust and fused to one another; together they form a posterior expansion where many muscles responsible for moving the femur in the hip joint were probably inserted.

The femur is slightly sigmoid and lacks a femoral crest; its length represents about 54% of the snout-vent length. The tibiofibula is somewhat shorter than the femur, whereas the length of the proximal tarsals is about 35% that of the tibiofibula. Fragments and incomplete impressions of the five metatarsals are preserved distal to the right tibiofibulare.

Comments on other specimens referred to Gracilisuchus avallei. The specimen MCCM-LH 17422 is of a slightly larger size (snout-vent length: 21.5 mm) than the holotype, although it is more poorly preserved and appears to be at a somewhat less advanced stage of development. It consists of a relatively complete, articulated individual split into part and counterpart. It probably belongs to an individual at the end of the metamorphosis, based on the incomplete fusion of distinct post sacral neural arches to the hypochord; and the still largely cartilaginous carpals and distal tarsals, although the distal phalanges are ossified in fore and hindlimbs. The overall shape of the azygous frontoparietal, wing-like nasals, general features of the vertebral column, and relative length of the metacarpals suggest that this specimen represents the same taxon than the holotype. If this is so, then this specimen provides additional information on some features, as discussed below.

Each nasal bears a short rostral process and has a concave anterior margin. The dorsal surface of the azygous frontoparietal is pierced by the pineal foramen at the level of the anterior third of the orbital length. A pair of circular depressions is clearly discernible on the ventral surface of the frontoparietal at the level of the posterior margin of the orbits; this feature might reflect the gross morphology of part of the brain but no thickenings that correspond to the cartilaginous structures of the endocranial roof are evident (Jarošová and Roček, 1982). Fragments and impressions of bones in the anterior palatal region are identified as representing the displaced vomers, the morphology of which can not be described in detail; however, it is evident that a row of 4–5 teeth is present on the ventral surface of each of these bones. As in the holotype, the presacral region of the vertebral column is about 62% of the median length of the skull. It is likely that six pairs of ribs were present during development, based on the evidence of fusion between ribs and transverse processes preserved in this specimen. The middle parts of the ribs are darker than their ends suggesting that mineralization started in the diaphyses and proceeded toward the epiphyses, as has been described in several extant taxa (Blanco and Sanchiz, 2000). In contrast with the other presacrals, the vertebra immediately preceding the sacrum has delicate, tapering transverse processes that are curved anteriorly.

The specimen MCCM-LH 11386 consists of an almost complete, articulated skeleton of a metamorphosing larva, the snout-vent length of which is estimated to have been about 16.5 mm (Fig. 7A). It is the earliest developmental stage represented among the specimens referred to *Gracilibatrachus avallei*. Most bones are preserved in ventral aspect, whereas a few elements are visible mainly as impressions. The azygous frontoparietal has an overall oval shape (Fig. 7C) that also characterizes metamorphosing or early juveniles of some extant and extinct xenoanurans (Trueb and Hanken, 1992; Roček, 2003b). As in MCCM-LH 17422, two rounded depressions that might be the impressions of parts of the brain can be observed on the ventral surface of the frontoparietal at the level of the anterior margin of the otic capsules (Fig. 7C). Premaxillae and maxillae are ossified, as well as dentaries and angulosplenials. A portion of the narrow cultriform process of the parasphenoid (Fig. 7C) is preserved attached to small fragments that probably belong to the sphenethmoid, a bone that might have started to ossify in the ventrolateral areas of the braincase. The prootics and exoccipitals form the prominent otic capsules; although these elements are crushed, no portion of the parasphenoid is evident on
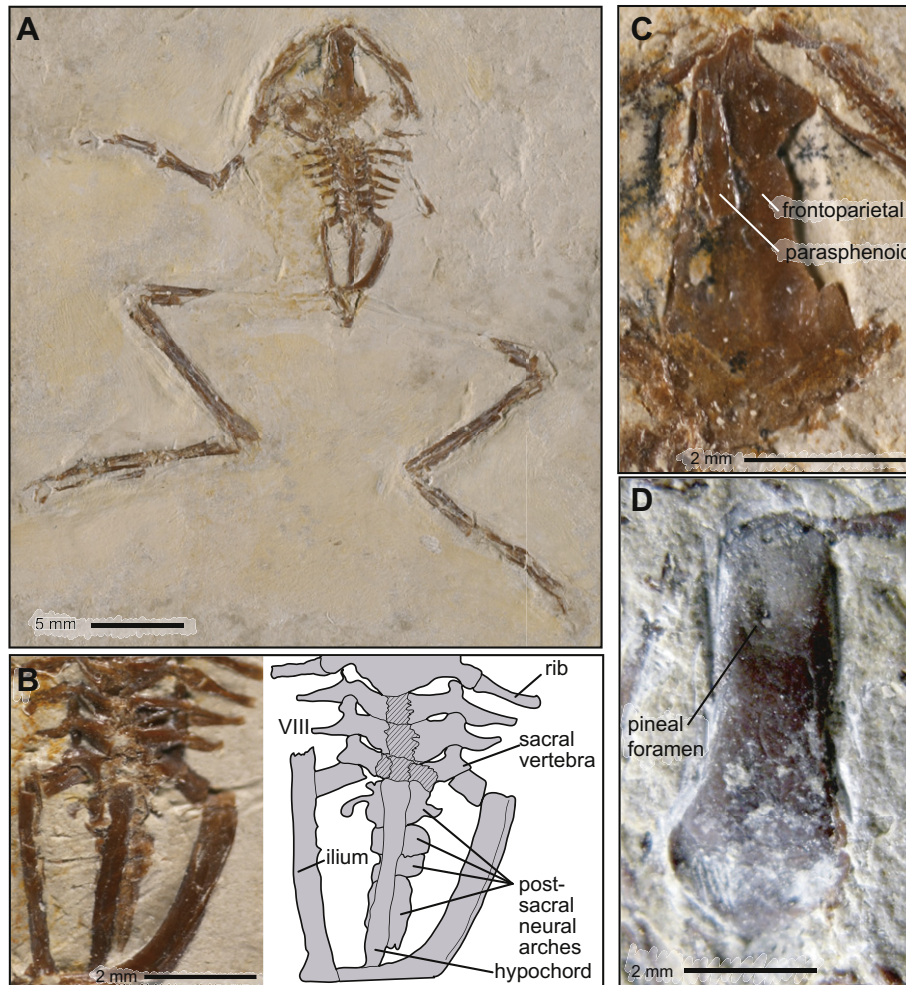
Fig. 7. *Gracilibatrachus avallei* gen. et sp. nov. A. MCCM-LH 11386, general aspect. B, Sacral region in ventral aspect; right, interpretive drawing. C, partial view of skull in ventral aspect. D, MCCM-LH 26803a, isolated frontoparietal in dorsal aspect.

their ventral surfaces. Seven presacrals are present; however, the most anterior of these vertebrae bear transverse processes articulated to ribs and, thus, probably represents Vertebra I + Vertebra II. The succeeding four vertebrae also bear transverse processes that are starting to fuse with the corresponding ribs. The transverse processes of the last two presacrals are the shortest of the entire vertebral column; those of Vertebra VII are laterally oriented, whereas the succeeding pair is slightly curved anteriorly. The vertebral centra of all presacral vertebrae are ossified, the last two weakly so. Relatively flat, rounded prezygapophyses are distinguishable; the positions of the prezygapophyses indicate that the neural arches were short and wide. The sacrum bears narrow diapophyses that are slanted posteriorly and the sacral centrum is not completely ossified. At least three separate ossified post sacral neural arches are visible, the most anterior of which bears short transverse processes. The hypochord is still separated from the dorsal part of the future urostyle (Fig. 4B). The radius and ulna are incompletely fused to one another. Elements of the carpus and tarsus are not preserved probably owing to their cartilaginous nature.

The specimen MCCM-LH 11387 consists of the articulated skeleton of a metamorphosing individual (snout-vent length: about 19 mm), preserved in ventral aspect; most bones are sectioned and a few are visible as impressions. The dorsal impression of the azygous frontoparietal shows that this bone was pierced anteriorly

by the pineal foramen, as in other specimens of this taxon. On both sides of the frontoparietal, at midlength of the orbits, occurs an elongated element that might be interpreted as a scletotic cartilage, which protects the eyeball. The vertebral column has eight presacrals; only the most posterior two vertebrae bear short, tapering transverse processes. There is evidence of at least one pair of transverse processes posterior to the sacral vertebra. An elongate impression posterior to the sacrum is interpreted as that of the hypochord which is not completely fused to the coccygeal elements.

The specimen MCCM-LH 26251 is also referable to *Gracilibatrachus avallei* based on its general proportions and morphology. It consists of a partially articulated skeleton, the snot-vent length of which is about 22 mm, preserved as pieces of bone and impressions. The pear-shaped, azygous frontoparietal, proportionally large otic capsules, and ribs not completely fused to the transverse processes suggest that it belongs to a juvenile individual.

The specimen MCCM-LH 26803a-b consists of three-dimensional, disarticulated remains that belong to more than one individual, preserved on two blocks as part and counterpart. It includes an azygous frontoparietal (Fig. 7D), otic capsules, and one scapula that are tentatively ascribed to this taxon based on their morphology and size, which agree closely with those of the specimens described above. The pineal foramen is visible near the anterior end of the frontoparietal. The bone has a median length of

about 6 mm, i.e., is nearly as long as those of the holotype and MCCM-LH 17422. The otic capsule, formed by the fused prootic and exoccipital, is exposed in ventral view and has a quadrangular overall shape. Anterior to the inflated inner ear region there is a depressed area that might have housed the Eustachian tube. The scapula that I tentatively assign to this taxon is partially preserved and exposed in dorsal view. The anterior edge is clearly straight owing to the presence of a thin web of bone (anterior lamina) between the shaft and the pars acromialis. The pars acromialis is slightly more expanded than the pars glenoidalis and is separated from the latter by a deep notch.

Isolated cross-sectioned vertebrae are also preserved on this slab. Two different morphological types can be discerned; these types differ mainly in the shape of the centrum, one being more rounded in cross section than the other. Both types, however, have notochordal canals, suggesting that ossification surrounded the notochord dorsally as well as ventrally; that is, it had a perichordal mode of centrum development. Because it is clear that some cranial bones associated with these vertebrae belong to *Gracilibatrachus avallei*, we assume tentatively that at least one of these morphotypes, probably the one with flattened centrum and high pedicels, belong to this species.

The specimen MCCM-LH 11394a, b is poorly preserved; it includes disarticulated cranial elements (large otic capsules, azygous frontoparietal, proportionally long sphenethmoid), as well as postcranial ones (partial vertebral column, bicondylar sacrum with narrow diapophyses, components of the pectoral girdle and forelimb, femur slightly longer than tibiofibula). It belongs to a postmetamorphic individual of an estimated snout-vent length of about 23 mm.

Remarks. All of the specimens described above are considered to represent a single species and have been referred to as "Las Hoyas 1" by Báez (in press); most of them belong either to tadpoles at advanced stages of metamorphosis or to recently metamorphosed individuals. The taxon represented by these specimens shares with members of Xenoanura the presence of an azygous frontoparietal and parasphenoid lacking subotic alae, two synapomorphies of this clade according to recent phylogenetic analyses (Báez et al., 2007; 2012). Xenoanura (=Pipoidea) is an "archaeobatrachian" (i.e., non-neobatrachian) monophyletic crown taxon comprised of the sister subclades Rhinophrynidae and Pipidae, a relationship recovered both in morphological (Cannatella, 1985; this paper) and molecular (Frost et al., 2006; Pyron and Wiens, 2011) phylogenetic analyses. As shown below, the extinct Palaeobatrachidae is internal to this clade, corroborating some previous studies (Ford and Cannatella, 1993; Henrici, 1998; Gao and Wang, 2001).

The shallow nasals and overall shape of the azygous frontoparietal of *Gracilibatrachus avallei* resemble the same elements of the only known specimen of *Neusibatrachus wilferti* from the early Barremian (formerly Berriasian–Valanginian) lacustrine limestones at La Pedrera, near Santa Maria de Meià in northeastern Spain. This specimen was originally described by Seiffert (1972) and probably belongs to a recently metamorphosed individual or an early juvenile (Báez and Sanchiz, 2007), the estimated snout-vent length of which is similar to those of the holotype of *G. avallei* and MCCM-LH 17422. The parasphenoid is not entirely preserved in any specimen of *G. avallei* examined; however, remnants of this bone make it evident that the cultriform process is narrow as is in *N. wilferti*. In addition, there is no evidence for the subotic extensions of the parasphenoid; moreover, the inflated inner ear region and the lack of scars left by the parasphenoid ala on a three-dimensionally preserved isolated otic capsule from Las Hoyas (MCCM-LH-26803) indicate that the parasphenoid lacks subotic alae in this taxon, as in *N. wilferti*. Apart from *Neusibatrachus*, comparisons of *Gracilibatrachus* are focused on several Mesozoic

pipimorphs, such as the mid Cretaceous *Thoraciliacus rostriceps* (Trueb, 1999) and *Cordicephalus gracilis* (Trueb and Báez, 2006) from Israel that were originally described by Nevo (1968), palaeobatrachids, and pipids.

The frontoparietal in *G. avallei*, as in *N. wilferti* and other xenoanurans, extends anteriorly to reach the nasals precluding the dorsal exposure of the sphenethmoid between these bones. The presence of a pineal foramen piercing the anterior portion of the well-ossified frontoparietal is a feature that characterizes some extinct and extant pipimorph xenoanurans (Báez and Trueb, 1997). In *N. wilferti* and *G. avallei* the premaxilla is relatively mediolaterally long and bears a blunt alary process directed toward the nasals, although this process appears to have a position closer to the midline of the skull in *N. wilferti*. The numbers of premaxillary and maxillary teeth are roughly similar in the two species and in both teeth are pedicellate with lingually curved crowns (Fig. 2E). Although in pipids with dentate upper jaws teeth are nonpedicellate (Trueb, 1996), pedicellate teeth have been described in the mid Cretaceous stem-pipid *Thoraciliacus* (Trueb, 1999), in a Berriasian putative pipimorph (Jones et al., 2003), as well as in a Jurassic basal rhinophrynid (Henrici, 1998). This evidence points to pedicelly as the primitive condition for xenoanurans. The presence of quadratojugal is not evident in any of the specimens of *G. avallei*, whereas this bone is present in the only known specimen of *N. wilferti*. An incomplete maxillary arch also occurs in pipimorphs for which this feature is known. There is no reliable evidence for the presence of mentomeckelian bones in *N. wilferti*, but these bones might have been present in *G. avallei*. Mentomeckelian bones are considered to be present in palaeobatrachids (Estes and Reig, 1973; Wuttke et al., 2012), although their presence in this group has been questioned (Cannatella and De Sá, 1993). These bones are lacking in other extinct and extant pipimorphs.

Paired dentate vomers, each bearing about five teeth in a single row occur in both *G. avallei* and *N. wilferti*. Well-developed, dentate vomers are also present in palaeobatrachids (Špinar, 1976; pers. obs.), whereas these bones lack teeth in rhinophrynids and in *Thoraciliacus rostriceps* (Trueb, 1999) and *Cordicephalus gracilis* (Trueb and Báez, 2006). In crown-group pipids the vomers are either reduced or absent (Cannatella and Trueb, 1988).

In *G. avallei*, a series of five vertebrae with long, distally blunt processes is present; in some specimens (MCCM-LH-21171) this series seems to be preceded by a short atlas that lacks transverse processes. In *N. wilferti* there are also five discrete vertebrae bearing distally blunt transverse processes that probably include ossified ribs, a feature that has been described also in Cainozoic palaeobatrachids (Roček, 2003b). This contrasts with the condition in other extinct and extant pipimorphs in which only three or four pairs of ribs have been documented during their development (e.g., Trueb and Hanken, 1992; Trueb and Báez, 2006; Báez et al., 2007). In *G. avallei*, the last two presacral vertebrae (VII and VIII) bear acuminate transverse processes, whereas in *N. wilferti* three vertebrae (VII–IX) with tapering processes are evident anterior to the sacrum (Báez and Sanchiz, 2007). The available evidence indicates that the only known specimen of *N. wilferti* has nine presacral vertebrae but it is not possible to know if this number of presacrals is the modal vertebral number or an intraspecific variant; in contrast, all specimens allocated in *Gracilibatrachus* have eight presacral vertebrae. The vertebral column of other xenoanurans is composed of eight or fewer presacrals.

In all specimens of *G. avallei* examined, the sacrum appears to be formed by a single vertebra, which has diapophyses that can be described as narrow because the distal length is about one-half their mediolateral width, and the sacro-urostylar articulation is bicondylar, resembling the corresponding conditions in *N. wilferti*. The narrow

sacral diapophyses contrast with the moderately to widely expanded diapophyses of pipimorphs for which the sacrum is known, including *Cordicephalus* (Trueb and Báez, 2006), *Thoraciliacus* (Trueb, 1999), and members of the crown group (Cannatella and Trueb, 1988). In addition, among xenoanurans a bicondylar articulation occurs only in rhinophrynids and palaeobatrachids, whereas in crown pipids the sacrum and urostyle are fused. In this regard, it is noteworthy that a monocondylar articulation between sacrum and urostyle has been described for *Thoraciliacus* (Trueb, 1999).

Transverse processes on the urostyle are not discernible in either the holotype of *G. avallei* or in that of *N. wilferti*, although in specimens that presumably belong to immature stages of the former the most anterior post sacral neural arch may bear a pair of transverse processes (Fig. 4B). A pair of reduced transverse processes on the urostyle is present in *Thoraciliacus rostriceps* (Trueb, 1999), whereas these elements are absent in *Cordicephalus* and pipids. Transverse processes may project from the urostyle during development in palaeobatrachids (Špinar, 1972; Roček, 2003b).

The pectoral girdle is not preserved well enough to make detailed comparisons to that of other taxa, but it is clear that the scapula of *Gracilibatrachus* resembles that of *N. wilferti* in general proportions and the presence of an anterior lamina along the leading edge. However, if the isolated scapula preserved in MCCM-LH-26803 belongs to *G. avallei*, a mediolaterally oriented notch separates the parts acromialis and glenoidalis as in many xenoanurans. This condition contrasts with the slightly indented scapula of *N. wilferti* (Báez and Sanchiz, 2007) and the uncleft scapula of palaeobatrachids and the extant pipid *Pipa*.

The long, straight, slightly proximally and distally expanded metacarpals of *G. avallei* are like those of *N. wilferti*, known mid Cretaceous pipimorphs (Nevo, 1968; Trueb, 1999; Báez et al., 2000; Trueb and Báez, 2006), palaeobatrachids (Špinar, 1972), and pipids (Trueb, 1996; Báez and Púgener, 2003). However, comparisons of the relative lengths of these bones with respect to the length of the radioulna in specimens of *G. avallei* of similar size to the only known specimen of *N. wilferti* show that these bones are somewhat proportionally shorter than in the latter species. The metacarpals are notably long in palaeobatrachids, in which these elements are as long as the radioulna.

The ilium of *G. avallei* bears a narrow dorsal crest along the shaft as that of *N. wilferti*; however, other comparisons with this species are difficult owing to the different position in which this bone is preserved in the available specimens of these taxa. A prominent dorsal crest on the iliac shaft is not evident in *Thoraciliacus* (Trueb, 1999), *Cordicephalus*, and *Avitabatrachus* (Báez et al., 2000; Báez et al., 2012). Unlike the living pipids, the ilium of *G. avallei* has a well-developed dorsal acetabular expansion (pars ascendens) that is exposed in acetabular view. This trait is also present in other Mesozoic putative pipimorphs (e.g., Estes and Sanchiz, 1982; Jones et al., 2003), probably denoting a less extensive interiliac synchondrosis than in living pipids.

In the specimens of *G. avallei* examined, the femur is slightly longer than the tibiofibula, except in MCCM-LH 11687 in which the relative lengths of these bones are reversed, whereas in *N. wilferti* the femur and the tibiofibula have a similar length. The femur is slightly longer than the tibiofibula in *Thoraciliacus*, *Cordicephalus* (Nevo, 1968), and palaeobatrachids (pers. obs.), but is shorter than the tibiofibula in some living pipids, such as *Silurana tropicalis*. Also, in *G. avallei* the proximal tarsals appear to be proportionally longer with respect to the snout-vent length than in *N. wilferti* (24% vs 17%).

Developmental aspects. The availability of individuals that belong to several developmental stages furnishes some evidence on different aspects of the skeletogenesis of *Gracilibatrachus avallei*, although because these specimens were not collected in association a description of the ossification sequence is not attempted. The least developed of the specimens referred to this taxon is MCCM-LH 11386, which has a skull lacking extensive ossification of the braincase in the orbital region (Fig. 7B). Likewise, ossification of the sphenethmoid occurs in relatively late metamorphic stages in palaeobatrachids (Roček, 2003b), the Palaeogene pipid *Llankibatrachus truebae* (Báez and Púgener, 2003), and the living pipid *Xenopus laevis* (Daudin) (Trueb and Hanken, 1992). The flat, pear-shaped frontoparietal of the same specimen resembles the gross morphology of this bone in metamorphosing tadpoles or juveniles of some extant and extinct pipimorph xenoanurans such as *Palaeobatrachus* (Roček, 2003b) and *Xenopus laevis* (Trueb and Hanken, 1992). In the same specimen from Las Hoyas the centra of the posterior presacral vertebrae appear less ossified than the most anterior ones, suggesting an anterior-posterior sequence of the ossification of the axial skeleton.

In MCCM-LH 11386, as in 11387, well-ossified, broad post sacral neural arches are distinguishable. In these two specimens the first post sacral element (X) bears transverse processes, whereas in the former this neural arch is followed by at least two distinct neural arch laminae. This suggests the participation of at least three post sacral vertebrae in the formation of the dorsal part of the anterior part of the urostyle in *G. avallei*. Among pipimorphs for which this information is available, three pairs of cartilaginous post sacral neural arches (corresponding to vertebrae X, XI, XII) have been recorded in the development of *X. laevis* (Pugener and Maglia, 2009), although a partial fourth pair (XIII) also may occur but is later reabsorbed (Smit, 1953: 107, 126). In this extant species, the post sacral neural arches are synchondrotically fused to each other in late metamorphosis and ossification takes place at the end of this event. Three post sacral neural arches, and occasionally a fourth one, have been also described in the development of *Palaeobatrachus* (Špinar, 1972; Roček, 2003b).

In *Gracilibatrachus avallei*, the coalescence of the ossified hypochord with the dorsal components of the anterior part of the urostyle might have occurred either at the end of the metamorphosis, as in *X. laevis*, or the hypochord might have remained distinct well after the end of the metamorphosis, as in *Palaeobatrachus*. The incomplete fusion of radius and ulna and tibia and fibula indicates a relatively late coalescence of these bones.

The presence of a notochordal canal, discernible in disarticulated vertebral centra (MCCM-LH 26803), might reflect immaturity; however, this evidence clearly indicates that the vertebral centra had a perichordal developmental mode, because in the epichordal mode the centrum does not ossify around the entire notochord (Mookerjee, 1931; Griffiths, 1963, Haas, 2003). This gives support to the hypothesis that perichordal vertebrae are plesiomorphic for xenoanurans, as proposed by Jones et al. (2003), and retained in rhinophrynids. The perichordal development of presacral vertebrae has also been suggested for the Berriasian putative basal pipimorph *Argyroua anoualensis* from Morocco (Jones et al., 2003) and the mid Cretaceous *Thoraciliacus* (Nevo, 1968). In contrast, in the Hauterivian pipimorph *Shomronella jordanica*, for which only tadpoles between Nieuwkoop and Faber stages 47 and 63 are known, the vertebral centra have been considered epichordal (Estes et al., 1978; Roček and van Dijk, 2006). However, although the ossification of the centra might have begun dorsal to the notochord in *Shomronella* ossifications ventral to and replacing the notochord, as well as lens-shaped intervertebral bodies, have been described for *Shomronella*. This suggests a developmental mode of centrum formation different from the epichordal mode described for the living pipid *Xenopus laevis* (Mookerjee, 1931; Smit, 1953).

4. Phylogenetic position of the new taxa

In order to estimate the phylogenetic position of *Gracilibatrachus avallei* and *Iberobatrachus angelae*, a maximum parsimony analysis based on the information derived from this study was performed with TNT version 1.1 (Goloboff et al., 2008). In this analysis terminal taxa included 16 extant species (Appendix A) representing major lineages within Anura according to current hypotheses of anuran relationships primarily based on molecular data (Frost et al., 2006; Pyron and Wiens, 2011). The taxon sample also included 8 fossil taxa, the age, geographic provenance, and putative phylogenetic position of which are relevant to the discussion of the Las Hoyas species relationships, as noted above. With regard to the characters, 72 osteological characters (Appendix B) were scored for the 24 taxa. Scoring of *Eodiscoglossus santonjae* was based on the examination of the holotype (MNCN 4723). These characters have been used in previous analyses (e.g., Báez et al., 2007; Báez et al., 2009 and literature cited therein), although some states were modified to make more explicit the way in which they were scored or to cover the variation in the present dataset. Autapomorphies of terminal taxa were omitted, as well as characters or states not present in the included taxa. All multistate characters were treated additively (unordered). The analysis of the matrix (Appendix C), previously prepared with Mesquite (Maddison and Maddison, 2010), was performed using the heuristic search with 500 random-addition sequences and tree bisection reconnection (TBR) branch swapping with a hold of 10. Three most parsimonious trees of 249 steps were generated under an assumption of equal weight, rooted on the extant *Ascaphus truei*. Additional searches under implied weights with a wide range of concavities (values of the constant k between 1 and 15) resulted in the tree shown in Fig. 8. A bootstrap analysis was also run in TNT with 1000 replicates to get some measure of node support. In the resulting trees, the crown-ward succession of Costata, Xenoanura, and Acosmanura was retrieved, although some of these groupings have little support. The present analysis supports the inclusion of

Iberobatrachus angelae within Costata. The monophyly of the latter group to the exclusion of *Eodiscoglossus santonjae*, however, is supported on one character only: the presence of opisthocoelous epichordal presacral vertebrae, a condition not possible to be ascertained in *I. angelae* based on the available evidence. Within this clade, it shares the presence of a squamosal-maxilla contact (ch 22, 1 → 2) and a palatine process on the maxilla (ch 14, 0 → 1) with the extant *Discoglossus*. The placement of the new taxon as a member of Costata and sister taxon of *Discoglossus* does not change even if a monophyletic *Alytes* + *Discoglossus* grouping, supported by molecular data, is enforced.

With regard to the position of *Gracilibatrachus avallei*, this taxon appears as a pipimorph xenoanuran based on several synapomorphies, such as short antorbital region (ch 1, 0 → 1), ankylosed ribs on anterior presacrals (ch 42, 2 → 1); columnar humerus (ch 60, 1 → 0) and elongated metacarpals (ch 63, 0 → 1). This position is also recovered in suboptimal trees one or two steps longer than the most parsimonious trees, although the internal topology of the clade formed by these xenoanuran taxa varies. *G. avallei* shares with other pipimorphs, except *Neusibatrachus wilferti*, the absence of a quadratojugal (ch 15, 0 → 1), whereas as in *Palaeobatrachus* the sternal end of the coracoid is expanded (ch 55, 0 → 1). The three most parsimonious trees differ in the relationships of *Gracilibatrachus*, which appears as the sister-taxon of *Neusibatrachus*, the sister-taxon of *Palaeobatrachus*, or between the latter two taxa, as successive sister-taxa of a clade that includes *Silurana*, *Thoraciliacus*, and *Cordicephalus* (Fig. 8). This analysis confirms the xenoanuran affinities of *Neusibatrachus* proposed in previous studies (Gao and Chen, 2004; Báez et al., 2007) but not the sister-taxon relationship of *Palaeobatrachus* and *Rhinophrynus* (Gao and Wang, 2001, Gao and Chen, 2004), although these studies differ from the present analysis in the taxon sampling and characters scored. The placement of *Palaeobatrachus* as a member of Pipimorpha obtained herein was also recovered by Henrici (1998); however, the inclusion of *Neusibatrachus* and *Gracilibatrachus* in the present analysis shows that some of the synapomorphies uniting Pipidae and Palaeobatrachidae listed by Henrici (1998), such as the elongate metapodials and presence of ribs, might support a more inclusive group of pipimorphs. *Gracilibatrachus avallei* lacks the derived features of palaeobatrachids (Wuttke et al., 2012) for which there is information in the available material, although the known features of this species are consistent with those that might be present in a basal member of this group. Interestingly, *Wealdenbatrachus* appears nested among neobatrachians, although this placement should be investigated further. To date, the oldest unquestionable neobatrachians are from the Aptian–Albian of northeastern Brazil (Báez et al., 2009) but the putative record of anomocoelans in Late Jurassic deposits of North America (Evans and Milner, 1993), if substantiated, sets a minimal divergence time for neobatrachians, according to our present understanding of anuran relationships. Likewise, corroboration of the taxonomic position of *Eodiscoglossus santonjae* requires an exhaustive revision of the several Jurassic and Cretaceous materials, some of which are fragmentary (e.g., Vergnaud-Grazzini and Wenz, 1975; Estes and Sanchiz, 1982), referred to this genus.

5. Discussion and conclusions

The present analysis supports the placement of *Iberobatrachus angelae* among costatans. Few osteological characters that optimize unambiguously on the branch leading up to the clade containing alytids and bombinatorids have been hitherto discovered, although the monophyly of Costata is supported by molecular data (Frost et al., 2006; Blackburn et al., 2010). Traditionally, the characterization of costatans has relied on a combination of plesiomorphic
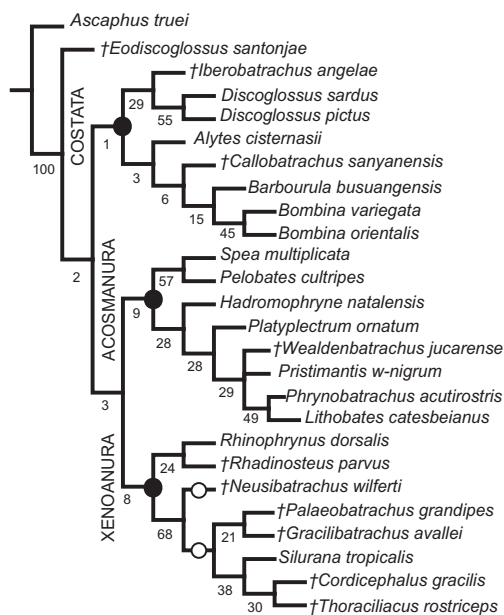

Fig. 8. One of the three most parsimonious trees obtained in the analysis of matrix shown in Appendix C, using the heuristic search of TNT v. 1.1 under assumption of equal weights. The other two trees differ in the placement of *Gracilibatrachus*, the alternate positions of which are indicated by the white circles. Fossil taxa are denoted with a †. Bootstrap absolute values (1000 replicates) are shown beside node points.

anuran traits (e.g., free ribs in adults, transverse processes on the urostyle) and putative derived features relative to leiopelmatids, the most basal living anurans (e.g., 8 presacral vertebrae instead of 9) (e.g., Lynch, 1973; Duellman and Trueb, 1986; Roček, 1994). The epichordal mode of vertebral centra development and, possibly, the opisthocoelous vertebrae have been considered as osteological synapomorphies that support the clade formed by the living taxa (Clarke, 1987, 2007; Haas, 2003; Frost et al., 2006). The poor preservation of the axial skeleton in the available specimens of *I. angelae* does not permit us to ascertain confidently the configuration of the vertebrae or estimate their developmental mode, although the possible presence of an anterior condyle in the centra of some anterior presacral vertebrae in MCCM-LH 15999 suggests opisthocoely.

Among the extant costatans, *I. angelae* differs clearly from bombinatorids in having mediolaterally shorter premaxillae, weaker coronoid processes on the angulosplenials, coracoids not posteriorly arched, and moderately expanded sacral diapophyses. The close relationship to *Discoglossus* retrieved herein is supported mainly by the presence of the palatine process on the maxilla and maxilla-squamosal contact. The homology of this maxillary process has been discussed thoroughly (Roček, 2003a; Banbury and Maglia, 2006) but it is still contentious; it is clear, however, that in the available specimens of *I. angelae* a discrete, free palatine (neopalatine of Trueb, 1993) is not present. Other features are also consistent with a relationship with *Discoglossus*, such as the well-ossified sphenethmoid that extends anterolaterally to form a process along the medial third of the otherwise cartilaginous antorbital plane, the narrow ventral flange on the anterior ramus of the pterygoid, and moderately expanded sacral diapophyses. However, it differs from the living genus in having a narrower neurocranium, posteriorly fused frontoparietals, more extensive pars facialis of the maxilla in the preorbital region, atlas lacking an intercotylar notch, and, probably, iliac shaft lacking a dorsal crest.

The present analysis did not retrieve the sister-taxa relationship of *Alytes* and *Discoglossus*, recovered in recent molecular phylogenies (Frost et al., 2006; Roelants et al., 2007; Pyron and Wiens, 2011). However, the placement of *Iberobatrachus* as a relative of *Discoglossus* implies that the divergence of this lineage from *Alytes* is a pre-Barremian event. This predates recent estimates that place this event in the late Early Cretaceous (Wiens, 2007; Blackburn et al., 2010), whereas, conversely, this result agrees with the timetrees of San Mauro et al. (2005) and Roelants et al. (2007) indicating a Late Jurassic split.

The placement of *Gracilibatrachus avallei* among xenoanurans is well supported by two synapomorphies: the azygous frontoparietal and parasphenoid lacking subotic alae. In addition, as in pipimorphs, but unlike rhinophrynids, the metacarpals are distinctively long, providing evidence that elongation of these bones, probably associated with an aquatic lifestyle, was an early trend in the history of this "archaeobatrachian" lineage. Moreover, the long distal manual phalanges in *G. avallei* add considerable length to the fingers, which might have been used for efficient scooping in aquatic feeding (Gray et al., 1997). With regard to other anatomical aspects, *G. avallei* is interesting because it has a bicondylar articulation between sacrum and urostyle as in palaeobatrachids and rhinophrynids, but unlike crown-group pipids, in which these elements are fused. However, it lacks the specialized synsacrum of palaeobatrachids, which includes at least Presacral VIII (Wuttke et al., 2012). It also has narrow sacral diapophyses, thus differing from the expanded, dorsoventrally compressed diapophyses of *Thoraciliacus*, *Cordicephalus*, and crown-group pipids.

Gracilibatrachus bears a general resemblance to *Neusibatrachus*, but comparisons between these taxa are limited because the latter is represented by a single, possibly juvenile, individual (Báez and Sanchiz, 2007). The quadratojugal is a dermal bone that, when present, appears at the end of the metamorphosis or shortly after. However, this bone is absent in specimens of *Gracilibatrachus* of similar size and degree of development to the holotype of *Neusibatrachus* or belonging to more mature stages. This appears significant in view that this bone is lacking in other pipimorphs. The description of these specimens as a separate genus and species rests mainly on these anatomical differences; a more complete understanding of the ontogenetic and individual variation of these taxa will permit a deeper insight on their taxonomic status and relationships.

Some skeletal features of *Gracilibatrachus* might be considered to be early steps in the evolution of a fully aquatic mode of life, a trend that culminates in palaeobatrachids and pipids. The relatively flat and wide head, short preorbital region of the skull, relatively short and compact vertebral column, particularly the presacral section, and long ischium are traits that might be associated with this lifestyle. However, the narrow sacral diapophyses and relatively long transverse processes of posterior presacral vertebrae indicate that a sliding joint between sacrum and ilium, advantageous for swimming (Emerson, 1979), was not present.

6. Paleobiogeographic significance

This study shows the inequivocal presence of costatans and pipimorph xenoanurans in the batrachofauna of northeast Spain in the Early Cretaceous. At this time this region was part of a plate that was becoming increasingly separate from Africa and North America by sea-floor spreading related to the opening of the central Atlantic and the neo-Tethys ocean (Ziegler, 1988; Schettino and Turco, 2011). Although available fossil records provide evidence, directly or indirectly, that costatan and pipimorph lineages had already differentiated by the earliest Cretaceous, there are practically no reports of anuran assemblages of this age containing representatives of both groups. It is, thus, interesting from a paleobiogeographic viewpoint that Jones et al. (2003) noted the possible pipimorph affinities of disarticulated bones from the Berriasian of Morocco associated with costatan (discoglossid therein) remains. In this regard, it is noteworthy that this possible pipimorph from north west Africa possesses the plesiomorphic state of several synapomorphies either of Gondwanan pipids or Laurasian palaeobatrachids, such as the narrow diapophyses of the monovertebral sacrum and the perichordal vertebral centra, like the pipimorphs from the Barremian of Spain (Báez and Sanchiz, 2007; this paper). The tectonic history of the Iberian Plate and its geographic proximity to the Tethyan margin of Gondwana in the earliest Cretaceous (Schettino and Turco, 2011) might account for a close biogeographic relationship between these areas, although discussion of the implications of these anuran records from this viewpoint awaits the unambiguous resolution of their relationships.

References

Báez, A. M. Salientia in Poyato-Ariza, F. J., Buscalioni, A. D., Fregenal-Martínez, M. A. (Eds.), Las Hoyas, a Cretaceous wetland. Verlag Dr. Friedrich Pfeil, München, in press.

Báez, A.M., Gómez, R.O., Taglioretti, M., 2012. The archaic ilial morphology of an enigmatic pipid frog from the upper Pleistocene of the South American pampas. Journal of Vertebrate Paleontology 32, 304–314.

Báez, A.M., Moura, G.J.B., Gómez, R.O., 2009. Anurans from the Early Cretaceous Crato Formation of northeastern Brazil: implications for the early divergence of neobatrachians. Cretaceous Research 30, 829–846.

Báez, A.M., Muzzopappa, P., Nicoli, L., 2007. Anurans from the Candeleros Formation (? Cenomanian-Turonian) of west-central Argentina: new evidence for pipoid evolution. Cretaceous Research 28, 1005–1016.

Báez, A.M., Púgener, L.A., 2003. Ontogeny of a new Palaeogene pipid frog from southern South America and xenopodinomorph evolution. Zoological Journal of the Linnean Society 139, 439–476.

Báez, A.M., Sanchiz, B., 2007. A review of Neusibatrachus wilferti, an Early Cretaceous frog from the Montsec Range, northeastern Spain. Acta Palaeontologica Polonica 52, 477–487.

Báez, A.M., Trueb, L., 1997. Redescription of the Paleogene Shelania pascuali and its bearing on the relationships of fossil and Recent pipoid frogs. Scientific Papers, Natural History Museum, The University of Kansas 4, 1–41.

Báez, A.M., Trueb, L., Calvo, J., 2000. The earliest known pipoid frog from South America: A new genus from the middle Cretaceous of Argentina. Journal of Vertebrate Palaeontology 20, 490–500.

Banbury, B., Maglia, A.M., 2006. Skeletal development of the Mexican spadefoot Spea multiplicata (AnuraÓ Pelobatidae). Journal of Morphology 267, 803–821.

Blackburn, D.B., Bickford, D.P., Diesmos, A.C., Iskandar, D.J., Brown, R.M., 2010. An ancient origin for the enigmatic flat-headed frogs (Bombinatoridae: Barbourula) from the islands of southeast Asia. Plos One 5, 1–10.

Blanco, M.J., Sanchiz, B., 2000. Evolutionary mechanisms of rib loss in anurans: A comparative developmental approach. Journal of Morphology 244, 57–67.

Bolkay, S.J., 1919. Osnove uporedne osteologije anurskih batrahija sa dodatkom o porijeklu Anura i sa slikom naravnoga sistema istih. Glasnik Zemaljskog Muzeja Bosni Hercegovini 31, 277–353.

Buatois, L.A., Mángano, M.G., Fregenal-Martínez, M.A., de Gibert, J.M., 2000. Short-term colonization trace-fossil assemblages in a carbonate-lacustrine Konservat-Lagerstätte (Las Hoyas fossil site, Lower Cretaceous, Cuenca, central Spain). Facies 43, 145–156.

Buscalioni, A.D., Fregenal-Martínez, M.A., 2010. A holistic approach to the palaeoecology of Las Hoyas Konservat-Lagerstätte (La Huérguina Formation, Lower Cretaceous, Iberian Ranges, Spain). Journal of Iberian Geology 36, 297–326.

Cannatella, D. C., 1985. A phylogeny of primitive frogs (Archaeobatrachians). Unpublished Doctoral Dissertation, University of Kansas, Lawrence.

Cannatella, D.C., De Sá, R.O., 1993. Xenopus laevis as a model organism. Systematic Biology 42, 476–507.

Cannatella, D.C., Trueb, L., 1988. Evolution of pipoid frogs: intergeneric relationships of the aquatic frog family Pipidae (Anura). Zoological Journal of the Linnean Society 94, 1–38.

Clarke, B.T., 1987. A description of Barbourula (Anura: Discoglossidae), with comments on its relationships. Journal of Natural History 21, 879–891.

Clarke, B.T., 2007. Comparative morphology and amphibian taxonomy: an example from the osteology of discoglossoid frogs. In: Heatwole, H., Tyler, M. (Eds.), Amphibian Biology 7. Surrey Beatty and Sons, Chipping Norton, pp. 2465–2612.

Duellman, W.E., Trueb, L., 1986. Biology of Amphibians. MacGraw-Hill Publishing Company, New York.

Emerson, S.B., 1979. The ilio-sacral articulation in frogs: form and function. Biological Journal of the Linnean Society 11, 153–168.

Estes, R., Reig, O.A., 1973. The early fossil record of frogs: a review of the evidence. In: Vial, J.L. (Ed.), Evolutionary Biology of the Anurans. Contemporary Research on Major Problems. University of Missouri Press, Columbia, pp. 11–36.

Estes, R., Sanchiz, B., 1982. Early Cretaceous lower vertebrates from Galve (Teruel) Spain. Journal of Vertebrate Paleontology 2, 21–39.

Estes, E., Špinar, Z.V., Nevo, E., 1978. Early Cretaceous pipid tadpoles from Israel (Amphibia: Anura). Herpetologica 34, 374–393.

Evans, S.E., McGowan, G.J., 2002. Lissamphibian remains from the Purbeck Limestone Group, southern England. In: Milner, A.R., Batten, D.J. (Eds.), Life and environments in Purbeck times. Special Papers in Palaeontology 68. The Palaeontological Association, London, pp. 103–119.

Evans, S.E., Milner, A., 1993. Frogs and salamanders from the Upper Jurassic Morrison Formation (Quarry Nine, Como Bluff) of North America. Journal of Vertebrate Paleontology 13, 24–30.

Fabrezi, M., Alberch, P., 1996. The carpal elements of anurans. Herpetologica 52, 188–204.

Fey, B., 1988. Die anurenfauna aus der Unterkreide von Uña (Ostspanien). Berliner Geowissensaftiche Abhandlungen 104 (A), 1–125.

Ford, L., Cannatella, D.C., 1993. The major clades of frogs. Herpetological Monographs 7, 94–117.

Fregenal-Martínez, M. A., Buscalioni, A. D., 2009. Las Hoyas konservat-lagersttäte: a field trip to a Barremian subtropical continental (wetland) ecosystem, in: Alcalá, L., Royo-Torres, R. (Coord.), Mesozoic Terrestrial Ecosystems in Eastern Spain, Fundamental 14, Fundación Conjunto Paleontológico de Teruel-Dinópolis, pp.133–152.

Frost, D.R., 2011. Amphibian Species of the World an Online Reference. Museum of Natural History, New York, USA. Version 5.5 (31 January, 2011). Electronic Database accessible at: http://research.amnh.org/vz/herpetology/amphibia/American.

Frost, D.R., Grant, T., Faivovich, J., Bain, R.H., Haas, A., Haddad, C.F.B., de Sá, R.O., Channing, A., Wilkinson, M., Donnellan, S.T., Raxworthy, C.J., Campbell, J.A., Blotto, B.L., Moler, P., Drewes, R.C., Nussbaum, R.A., Lynch, J.D., Green, D.M., Wheeler, W.C., 2006. The Amphibian Tree of Life. Bulletin of the American Museum of Natural History 297, 1–370.

Gao, K.-Q., Wang, Y., 2001. Mesozoic anurans from Liaoning Province, China, and phylogenetic relationships of archaeobatrachian anuran clades. Journal of Vertebrate Paleontology 21, 460–476.

Gao, K.-Q., Chen, S., 2004. A new frog (Amphibia, Anura) from the Lower Cretaceous of western Liaoning, China. Cretaceous Research 25, 761–769.

Goloboff, P., Farris, J., Nixon, K., 2008. T.N.T., a free program for phylogenetic analysis. Cladistics 24, 774–786.

Gómez Fernández, J.C., Meléndez, N., 1991. Rithmically laminated lacustrine carbonates in the Lower Cretaceous of La Serranía de Cuenca Basin (Iberian Ranges, Spain). In: Anadón, P., Cabrera, L.L., Kelts, K. (Eds.), Lacustrine Facies Analysis. Special Publication of the International Association of Sedimentologists 13, pp. 245–256.

Gray, L.A., O'Reilly, J.C., Nishikawa, K.C., 1997. Evolution of forelimb movement patterns for prey manipulation in anurans. Journal of Experimental Zoology 277, 417–424.

Griffiths, I., 1963. The phylogeny of the Salientia. Biological Reviews 38, 241–292.

Haas, A., 2003. Phylogeny of frogs as inferred primarily on larval characters (Amphibia, Anura). Cladistics 19, 23–89.

Hecht, M.K., 1970. The morphology of Eodiscoglossus, a complete Jurassic Frog. American Museum Novitates 2424, 1–17.

Henrici, A., 1998. A new pipoid anuran from the Late Jurassic Morrison Formation at Dinosaur Nacional Monument, Utah. Journal of Vertebrate Paleontology 18, 321–332.

Jarošová, J., Roček, Z., 1982. The incrassatio frontoparietalis in frogs, its origin and phylogenetic significance. Amphibia-Reptilia 3, 111–124.

Jones, M.E.H., Evans, S.E., Sigogneau-Russell, D., 2003. Early Cretaceous frogs from Morocco. Annals of the Carnegie Museum 72, 65–97.

Lynch, J.D., 1971. Evolutionary Relationships, Osteology, and Zoogeography of Leptodactyloid Frogs. University of Kansas Museum of Natural History Miscellaneous Publication 53. 1–238.

Lynch, J.D., 1973. The transition from archaic to advanced frogs. In: Vial, J.L. (Ed.), Evolutionary Biology of the Anurans. Contemporary Research on Major Problems. University of Missouri Press, Columbia, pp. 131–182.

Maddison, W.P., Maddison, D.R., 2010. Mesquite: A Modular System for Evolutionary Analysis. Version 2.74. Available at: mesquiteproject.org/mesquite/download/download.html.

Maglia, A.M., Pugener, L.A., 1998. Skeletal development and adult osteology of Bombina orientalis (Anura: Bombinatoridae). Herpetologica 54, 344–363.

Mookerjee, H.K., 1931. On the development of the vertebral column in Anura. Philosophical Transactions of the Royal Society of London B 219, 165–196.

Nevo, E., 1968. Pipid frogs from the Early Cretaceous of Israel and pipid evolution. Bulletin of the Museum of Comparative Zoology, Harvard University 136, 255–318.

Pugener, L.A., Maglia, A.M., 1997. Osteology and skeletal development of Discoglossus sardus (Anura: Discoglossidae). Journal of Morphology 233, 267–286.

Pugener, L.A., Maglia, A.M., 2007. Skeletal morphology and development of the olfactory region of Spea (AnuraÓ Scaphiopodidae). Journal of Anatomy 211, 754–768.

Pugener, L.A., Maglia, A.M., 2009. Developmental evolution of the anuran sacrourostylic complex. South American Journal of Herpetology 4, 193–209.

Pyron, R.A., Wiens, J.J., 2011. A large-scale phylogeny of Amphibia including over 2800 species, and a revised classification of extant frogs, salamanders, and caecilians. Molecular Phylogenetics and Evolution 61, 543–583.

Ritland, R.M., 1955. Studies on the pos-cranial morphology of Ascaphus truei. I. skeleton and spinal nerves. Journal of Morphology 97, 119–177.

Roček, Z., 1980. Cranial anatomy of frogs of the family Pelobatidae Stannius, 1856, with outlines of their phylogeny and systematics. Acta Universitatis Carolinae Biologica 1-2, 1–164.

Roček, Z., 1994. Taxonomy and distribution of the Tertiary discoglossids (Anura) of the genus Latonia V. Meyer, 1843. Geobios 27, 717–751.

Roček, Z., 2000. Mesozoic anurans. In: Heatwole, H., Carroll, R.L. (Eds.), Amphibian Biology 4. Surrey Beatty and Sons, Chipping Norton, New South Wales, pp. 1295–1351.

Roček, Z., 2003a. Larval development and evolutionary origin of the anuran skull. In: Heatwole, H., Davies, M. (Eds.), Amphibian Biology 5. Surrey Beatty and Sons, Chipping Norton, New South Wales, pp. 1878–1995.

Roček, Z., 2003b. Larval development in Oligocene palaeobatrachid frogs. Acta Palaeontologica Polonica 48, 595–607.

Roček, Z., van Dijk, E., 2006. Patterns of larval development in Cretaceous pipid frogs. Acta Palaeontologica Polonica 51, 111–126.

Roelants, K., Gower, D.J., Wilkinson, M., Loader, S.P., Biju, S.D., Guillaume, K., Moriau, L., Bossuyt, F., 2007. Global patterns of diversification in the history

of modern amphibians. Proceedings of the Academy of Sciences. USA 104, 887—892.

Sanchiz, B., 1998. Salientia. In: Wellnhofer, P. (Ed.), Encyclopedia of Paleoherpetology. Verlag Dr. Friedrich Pfeil, München, pp. 1—275.

San Mauro, D., Vences, M., Alcobendas, M., Zardoya, R., Meyer, A., 2005. Initial diversification of living amphibians predated the breakup of Pangaea. The American Naturalist 165, 590—599.

San Mauro, D., 2010. The multilocus timescale for the origin of extant amphibians. Molecular Phylogenetics and Evolution 56, 554—561.

Sanz, J.L., Wenz, S., Yébenes, A., Estes, R., Martínez-Delclòs, X., Jiménez-Fuentes, E., Diéguez, C., Buscalioni, A.D., Barbadillo, L.J., Vía, L., 1988. An Early Cretaceous faunal and floral continental assemblage: Las Hoyas fossil site (Cuenca, Spain). Geobios 21, 611—635.

Savage, J.M., 1973. The geographic distribution of frogs: patterns and predictions. In: Vial, J.L. (Ed.), Evolutionary Biology of the anurans: contemporary research on major problems. University of Missouri Press, Columbia, pp. 351—445.

Schettino, A., Turco, E., 2011. Tectonic history of the western Tethys since the Late Triassic. Bulletin of the Geological Society of America 123, 89—105.

Seiffert, J., 1972. Ein Vorläufer der froschfamilien Palaeobatrachidae und Ranidae im Greinzbereich Jura-Kreide. Neues Jahrbuch der Mineralogie, Geologie, und Paläontologie 1972, 120—131.

Smit, A.L., 1953. The ontogenesis of the vertebral column of Xenopus laevis (Daudin) with special reference to the segmentation of the metotic region of the skull. Annals of the University of Stellenbosch 29, 79—136.

Špinar, Z.V., 1972. Tertiary frogs from Central Europe. Academia, Publishing House of the Czechoslovak Academie of Sciences, Prague, 286 pp.

Špinar, Z.V., 1976. The hyoid apparatus and vomers in palaeobatrachids (Anura). Věstník Ústředního ústavu geologického 51, 179—183.

Szentesi, Z., Venczel, M., 2012. A new discoglossid frog from the Upper Cretaceous (Santonian) of Hungary. Cretaceous Research 34, 327—333.

Talavera, R.R., 1990. Evolución de pelobátidos y pelodítidos (Amphibia, Anura) Ó Morfología y desarrollo del sistema esquelético. Doctoral Dissertation 188/90, Editorial de la Universidad Complutense, Madrid.

Trueb, L., 1973. Bones, frogs and evolution. In: Vial, J.L. (Ed.), Evolutionary Biology of the Anurans. Contemporary Research on Major Problems. University of Missouri Press, Columbia, pp. 65—132.

Trueb, L., 1993. Patterns in cranial diversity among the Lissamphibia. In: Hanken, J., Hall, B.K. (Eds.), The Vertebrate SkullÓ Patterns of Structural Systematic Diversity, vol. 2. University of Chicago Press, Chicago, pp. 255—343.

Trueb, L., 1996. Historical constraints and morphological novelties in the evolution of the skeletal system of pipid frogs (Anura: Pipidae). In: Tinsley, R.C., Kobel, H.R. (Eds.), The Biology of Xenopus. Oxford University Press, pp. 349—377.

Trueb, L., 1999. The Early Cretaceous pipoid frog Thoraciliacus: redescription, revaluation, and taxonomic status. Herpetologica 55, 139—157.

Trueb, L., Báez, A.M., 2006. Revision of the Early Cretaceous Cordicephalus from Israel and an assessment of its relationships among pipoid frogs. Journal of Vertebrate Paleontology 26, 44—59.

Trueb, L., Cannatella, D.C., 1982. Osteology and laryngeal apparatus of Rhinophrynus dorsalis (Anura: Rhinophrynidae) with comparisons to recent pipid frogs. Journal of Morphology 171, 11—40.

Trueb, L., Hanken, J., 1992. Skeletal development in Xenopus laevis (Anura, Pipidae). Journal of Morphology 214, 1—41.

Vergnaud-Grazzini, C., Wenz, S., 1975. Les discoglossidés du Jurassique Supérieur du Monsech (Province de Lérida, Espagne). Annales de Paléontologie (Vertébrés) 61, 19—36.

Wang, Y., Gao, K.-Q., 1999. Earliest Asian discoglossid from western Liaoning. Chinese Science Bulletin 44, 636—642.

Wiens, J.J., 2007. Global patterns of diversification and species richness in amphibians. The American Naturalist 170, S86—S106.

Wuttke, M., Přykyl, T., Ratnikov, V., Dvořák, Z., Roček, Z., 2012. Generic diversity and distributional dynamics of the Palaeobatrachidae (Amphibia: Anura). Senckenberg Gesellschaft für Naturforschung and Springer. Published on line: http://dx.doi.org/10.1007/s12549-012-0071-.

Ziegler, P.A., 1988. Evolution of the Arctic-North Atlantic and the Western Tethys. American Association of Petroleum Geologists Memoir 43, 1—198.

Appendix A

Specimens of extant taxa examined for the osteological comparisons and phylogenetic analysis. Abbreviations: LD, data taken from literature, source in brackets; CS, cleared and stained; DS, dry skeleton; AMNH, American Museum of Natural History; FCEN, Facultad de Ciencias Exactas y Naturales de la Universidad de Buenos Aires; KU, Museum of Natural History, University of Kansas; MACN, Museo Argentino de Ciencias Naturales "Bernardino Rivadavia"; MCN, Museo de Ciencias Naturales de la Universidad Nacional de Salta; MNCN, Museo Nacional de Ciencias Naturales de Madrid; UN, unnumbered specimen:

Leiopelmatidae
Ascaphus truei Stejneger, 1899, AMNH 176858, DS; AMNH 20656, DS., AMNH 57969, CS; LD (Ritland, 1955)
Costata
Alytidae: *Alytes cisternasii* Boscá, 1879, FCEN-P, UN, DS; *Discoglossus pictus* Otth, 1837, FCEN-P, UN, CS& DS; KU 148657, DS; *Discoglossus sardus* Tschudi, 1837, LD (Pugener and Maglia, 1997)

Bombinatoridae: *Bombina variegata* (Linnaeus, 1758) MCN 810, CS, AMNH 37528, DS; FCEN-V 401, DS; *Bombina orientalis* (Boulenger 1890), MNCN 16245, CS, LD (Maglia and Pugener, 1998); *Barbourula busuangensis* Taylor and Noble, 1824, KU 79003, DS., LD (Clarke, 1987)
Xenoanura
Rhinophrynidae: *Rhinophrynus dorsalis* Dumeril and Bibron 1841, MACN 42617, DS, LD (Trueb and Cannatella, 1982)
Pipidae: *Silurana tropicalis* Gray, 1864, MACN 42633, DS
Anomocoela
Pelobatidae: *Pelobates cultripes* (Cuvier, 1829), MACN 42619, CS, LD (Talavera, 1990)
Scaphiopodidae: *Spea multiplicata* (Cope, 1863), LD (Banbury and Maglia, 2006; Pugener and Maglia, 2007)
Neobatrachia
Heleophrynidae: *Hadromophryne natalensis* (Hewitt, 1913), KU195926, CS.
Hyloides
Limnodynastidae: *Platyplectrum ornatum* (Gray, 1842), MACN 42620, DS
Strabomantidae: *Pristimantis w-nigrum* (Boettger, 1892), KU 190094, DS.
Ranoides
Phrynobatrachidae: *Phrynobatrachus acutirostris* Nieden, 1913, MCN 951, CS.
Ranidae: *Lithobates catesbeianus* (Shaw, 1802), FCEN-P, UN, DS.

Appendix B

List of characters
Cranial characters
(1) Preorbital region, relative length: (0) one-third, or more, of the skull length; (1) one-quarter, or less, of the skull length.
(2) Nasals, relationship to one another: (0) broadly separated; (1) narrowly separated or sutured.
(3) Frontoparietals, relationship with nasals: (0) not in contact; (1) in contact.
(4) Frontoparietals, relationship to one another: (0) separate throughout most of their lengths; (1) posteromedial margins close or in contact, diverging only anteriorly; (2) sutured throughout length; (3) completely fused or azygous.
(5) Frontoparietals, supraorbital flange: (0) absent; (1) present.
(6) Pineal foramen: (0) absent; (1) present.
(7) Sphenethmoid, configuration: (0) right and left elements dorsally and ventrally separated; (1) dorsally separated; (2) girdle-bone.
(8) Sphenethmoid, dorsal exposure: (0) present; (1) absent.
(9) Optic foramina, margins: (0) bound in cartilage or cartilage and bone; (1) bound completely in bone.
(10) Postnasal wall, ossification: (0) completely cartilaginous or ossified/mineralized less than one-half; (1) ossified/mineralized more than one-half.
(11) Perilymphatic foramina, position respect to jugular foramen (0) inferior and superior anterior; (1) inferior posterior, superior anterior; (2) both posterior
(12) Prootic, Eustachian canal: (0) absent; (1) present.
(13) Maxilla, preorbital process: (0) absent or weakly developed; (1) well developed.
(14) Maxilla, pars facialis, palatine process: (0) absent; (1) present.
(15) Quadratojugal: (0) present; (1) absent.
(16) Vomer: (0) present; (1) absent.
(17) Vomer, plate-like anterior portion: (0) absent or poorly developed; (1) well-developed.
(18) Vomer, postchoanal process: (0) absent; (1) present.
(19) Palatine: (0) absent; (1) present.
(20) Parasphenoid, subotic alae: (0) present; (1) absent.
(21) Parasphenoid, cultriform process, anterior extent: (0) not reaching maxillary arch; (1) reaching maxillary arch.
(22) Squamosal, zygomatic ramus: (0) reduced or absent; (1) moderately to well developed, free-ending; (2) well developed, articulating with maxilla; (3) well developed, articulating with pterygoid.
(23) Squamosal, otic ramus: (0) poorly to moderately developed, medial process poorly differentiated or absent; (1) present, with distinct medial process that rests on the crista parotica; (2) present, with extensive medial process that rests on the otoccipital.
(24) Crista parotica, condition: (0) mostly cartilaginous; (1) mineralized.
(25) Occipital artery, location: (0) dorsal to skull roof; (1) housed in a closed canal.
(26) Pterygoid, medial ramus, contact with parasphenoid: (0) absent; (1) present.
(27) Pterygoid, anterior ramus, length: (0) short to moderate, anterior end well posterior to the antorbital plane; (1) long, reaching or nearly, the antorbital plane.
(28) Angulosplenial, coronoid process: (0) low, poorly developed; (1) well developed, but short; (2) long, blade-like.
(29) Mentomeckelian bone: (0) present; (1) absent.
(30) Jaw articulation, position: (0) lateral to the otic capsule; (1) at the anterolateral corner of the otic capsule.
Characters of the hyobranchial apparatus
(31) Hyoid apparatus, posteromedial process, anterior end: (0) wider than posterior end; (1) equally developed or narrower than posterior end.
(32) Hyoid apparatus, parahyoid bone: (0) present; (1) absent.
(33) Hyoid apparatus, hyale general configuration: (0) complete; (1) incomplete.
Postcranial characters
(34) Presacral vertebrae, number: (0) nine; (1) eight; (2) seven (eighth vertebra incorporated into the sacrum).

(35) Atlas, cotyle configuration: (0) closely juxtaposed (including a single articulation facet); (1) well separated (type I of Lynch, 1971).
(36) Vertebral centra, formation pattern: (0) perichordal; (1) epichordal.
(37) Last presacral vertebra, configuration of centrum according to articulation facets: (0) notochordal; (1) opisthocoelous; (2) procoelous; (3) amphicoelous.
(38) Posterior presacral vertebrae (except last presacral), posteromedial margin of neural arch: (0) slightly concave to straight or with a minute neural spine; (1) projecting in a well-developed neural spine.
(39) Vertebra VI, transverse processes, proximal-distal length in comparison to sacral length: (0) shorter; (1) nearly equal.
(40) Presacral vertebrae I and II: (0) not fused, weak or no imbrication; (1) not fused, broad imbrication medially only; (2) not fused, broad imbrication involving all the neural laminae; (3) synostotically fused; (4) synchondrotically fused.
(41) Vertebra VI, orientation of posterior margin of transverse processes with respect to axial axis: (0) nearly perpendicular; (1) moderately forward; (2) markedly forward: (3) posterior.
(42) Ribs on anterior presacrals: (0) free bony ribs present in larvae and adults; (1) free bony ribs present in larvae and ankylosed to transverse processes in adults; (2) free bony ribs absent in larvae and adults.
(43) Sacrum and urostyle, articulation: (0) non-synovial; (1) synovial, monocondylar; (2) synovial, bicondylar; (3) synchondrotically or synostotically fused.
(44) Sacral diapophyses, distal cross-section: (0) flattened; (1) nearly round
(45) Sacral diapophyses, distal expansion as ratio of distal length and mediolateral width: (0) widely expanded (ratio ≥ 1.5); (1) moderately expanded (1.5 > ratio > 0.75); (2) weakly expanded or unexpanded (ratio < 075).
(46) Sacral diapophyses, distal margin in dorsal view: (0) laterally convex; (1) straight
(47) Sacral diapophyses, anterior margin orientation in dorsal view: (0) nearly horizontal; (1) anterior; (2) posterior.
(48) Urostyle, transverse processes: (0) present; (1) absent.
(49) Urostyle, dorsal ridge: (0) absent, inconspicuous or low; (1) present, moderately to well developed.
(50) Clavicle, relation to scapula: (0) lateral end contacts medial edge of pars acromialis; (1) lateral end overlaps anterior edge of pars acromialis; (2) lateral end is fused to scapula.

(51) Scapula, proportions: (0) glenoid area one-third, or less, total length; (1) glenoid area more than one-third total length.
(52) Scapula, relative length: (0) shorter than clavicle; (1) longer than clavicle; (2) nearly as long as clavicle.
(53) Scapula, anterior lamina: (0) present; (1) absent.
(54) Cleithrum, distal end: (0) not forked; (1) forked.
(55) Coracoid, sternal expansion relative to coracoid length: (0) sternal expansion less than half the length of the coracoid; (1) sternal expansion nearly half the length of the coracoid; (2) sternal expansion nearly the length of the coracoid.
(56) Omosternum: (0) present; (1) absent.
(57) Omosternum, condition: (0) cartilaginous; (1) ossified, not forked; (2) ossified, forked.
(58) Sternum: (0) present; (1) absent.
(59) Sternum, condition: (0) cartilaginous; (1) ossified.
(60) Humerus, shaft: (0) columnar; (1) ventrally curved.
(61) Post axial carpals (ulnare, distal carpals 3, 4, and 5): (0) all discrete; (1) distal carpals 4 and 5 fused; (2) distal carpals 3, 4, and 5 fused.
(62) Carpal torsion: (0) absent; (1) present.
(63) Metacarpals, length: (0) relatively short, not longer than 60 % of radioulna length; (1) long, longer than 70 % of radioulna length.
(64) Ilium, spiral groove on shaft: (0) absent; (1) present.
(65) Ilium, dorsal crest on shaft: (0) absent; (1) present as a low ridge; (2) well developed as a flange (wider than one-half of the shaft width).
(66) Interiliac scar: (0) absent to narrow; (1) ample, but restricted to ventral part of ilia; (2) ample both ventrally and dorsally.
(67) Angle between the margin of the ventral acetabular expansion and the ventral margin of the iliac shaft in acetabular view: (0) acute; (1) nearly right; (2) obtuse.
(68) Ischium, shape in lateral view: (0) long, with a nearly rectangular outline; (1) short, with semicircular outline.
(69) Pubis, condition: (0) cartilaginous; (1) partially or completely ossified.
(70) Tibiofibula, length in relation to femur length: (0) shorter; (1) subequal; (2) longer.
(71) Prehallux, distal bone: (0) not modified; (1) modified into a spade.
(72) Distal tarsals 2 and 3: (0) separate; (1) fused.

Appendix C

Data matrix of the 72 characters coded among the 26 taxa. Symbols: A = (01); B = (02); ? = missing data or inapplicable.

	10	20	30	40	50	60	70	
Ascaphus truei	00A0000000	0000100000	0100000000	0000000000	300020B001	10?111?001	000000?112	00
Alytes cisternasii	0101002000	1000001100	0001000100	?001011001	0020101001	1200000001	0000002101	00
Barbourula busuangensis	11120021?0	?010001100	01010?0?02	00010?1002	1010011001	1000000000	100001200?	00
Bombina orientalis	0101002000	1000001100	0100001100	1001011003	1010001001	1000000?00	0001012101	0?
Bombina variegata pachypus	0101002000	1000001100	0100001100	1001011001	1010001001	1000000?00	000?012100	00
Callobatrachus sanyanensis†	01??0?2000	????0011??	?10?0?1?00	???0?11?01	102???10?1	??01?????1	0?0?1?1??1	0?
Cordicephalus gracilis†	11130??111	?11?101001	11?0000010	0??1?11004	0130101101	100?0????0	0?1001??10	0?
Discoglossus pictus	0111002000	1001001100	0211000100	0001011101	1020100001	1000100000	0000201102	00
Discoglossus sardus	0101002000	?001001100	0211000100	??01011102	0020100001	1200100000?	000020210?	00
Eodiscoglossus santonjae†	0101?0?0?0	?0??00????	?1?1??0??0	???1???00?	00??2?2??1	???1??????	000??????1	0?
Gracilibatrachus avallei†	11130121?0	?10010??01	?100?00000	???100?00?	01202?21?1	1000?1????0	0?1?1????0	0?
Hadromophryne natalensis	0000002000	?010000110	0110000100	0101002002	3220200100	1000000001	010000??02	01
Iberobatrachus angelae†	010?0?2000	?01100110?	?2?1??0000	???10???0?	00?01?20??	1?000????0	?00?0????2	0?
Lithobates catesbeianus	0112002000	2010001110	0011010102	?101003111	32212?2110	1111201011	2100201001	01
Neusibatrachus wilferti†	11130??100	??0?00??01	?1?0?00000	?0?00?2004	01202?22?1	100?0????0	??1?1???01	0?
Palaeobatrachus grandipes†	11130?2100	1100101101	1100001001	?0?2012004	012010?101	10001????0	??10112?10	0?
Pelobates cultripes	0113102001	1001001100	0221110000	0111012101	2210011100	0100100011	0101002100	10
Phrynobatrachus acutirostris	0012000?000	?010000110	0110000100	1101?3010	32212?2110	1101201011	210020??02	01
Platyplectrum ornatum	0000002000	2010000?110	0111101100	1101002103	12201?2110	0111000000	1100101101	11
Pristimantis w-nigrum	0102002000	2010001110	0111011?00	1101112010	32212?0112	0210000000?	210020?112	01
Rhadinosteus parvus†	???3?0????	?00??????1	??????????	???1003???	??2????1?1	1010??????	??0?002??1	??
Rhinophrynus dorsalis	0113102101	1000001101	0001000001	0011003102	0220100111	120111?1?1	0100002100	11
Silurana tropicalis	1113011110	?10011??01	1311001210	1101111003	2130011102	10?001?000	0110122012	01
Spea multiplicata	0101002001	1001101100	01111A0000	111100B001	2230101100	0110000001	0101002100	11
Thoraciliacus rostriceps†	1113?1?110	?01?1?0?01	11?0000010	???1001004	0110101001	12??0????0	0?1?01??10	00
Wealdenbatrachus jucarense†	0?0100????	????0????0	011??10??0	???????11?	302??2010	0?1?0????1	??0020?1?2	??